



Review

Tuneable Lenses Driven by Dielectric Elastomers: Principles, Structures, Applications, and Challenges

Zhuoqun Hu ^{1,2}, Meng Zhang ^{1,2}, Zihao Gan ^{1,2}, Jianming Lv ^{1,2}, Zhuoyu Lin ^{1,2} and Huajie Hong ^{1,2,*}

- College of Intelligence Science and Technology, National University of Defense Technology, Changsha 410073, China; hzq_nudt304@163.com (Z.H.)
- National Key Laboratory of Equipment State Sensing and Smart Support, National University of Defense Technology, Changsha 410073, China
- * Correspondence: opalqq@163.com

Abstract: As the core element of adaptive optical systems, tuneable lenses are essential in adaptive optics. Dielectric elastomer-driven tuneable lenses offer significant advantages in tuning range, response speed, and lightweight design compared to traditional mechanical zoom lenses. This paper systematically reviews the working mechanisms and research advancements of these lenses. Firstly, based on the two driving modes of deformation zoom and displacement zoom, the tuning principle of dielectric elastomer-driven tuneable lenses is analysed in depth. Secondly, the design methodology and current status of the research are systematically elaborated for four typical structures: monolithic, composite, array, and metalenses. Finally, the potential applications of this technology are discussed in the fields of auto-zoom imaging, microscopic imaging, augmented reality display, and infrared imaging, along with an analysis of the key technological challenges faced by this technology, such as material properties, modelling and control, preparation processes, and optical performance. This paper aims to provide a systematic reference for researchers in this field and to help promote the engineering application of dielectric elastomer tuneable lens technology.

Keywords: tuneable lenses; dielectric elastomers; liquids; soft solids; review



Academic Editor: Ephraim Suhir

Received: 22 May 2025 Revised: 16 June 2025 Accepted: 17 June 2025 Published: 19 June 2025

Citation: Hu, Z.; Zhang, M.; Gan, Z.; Lv, J.; Lin, Z.; Hong, H. Tuneable Lenses Driven by Dielectric Elastomers: Principles, Structures, Applications, and Challenges. *Appl. Sci.* 2025, *15*, 6926. https://doi.org/ 10.3390/app15126926

Copyright: © 2025 by the authors. Licensee MDPI, Basel, Switzerland. This article is an open access article distributed under the terms and conditions of the Creative Commons Attribution (CC BY) license (https://creativecommons.org/ licenses/by/4.0/).

1. Introduction

As one of the core components of modern optical technology, zoomable optical systems play an essential role in many fields such as biomedicine [1], industrial production [2], military security [3], and consumer electronics [4]. Traditional zoomable optical systems are usually made of solid materials such as glass and plastic with fixed-focus lenses, and their zoom is often achieved by multiple solid lenses with mechanical devices [5,6]. With the continuous expansion of application scenarios, the lightweight, responsive, and low-cost performance requirements of zoomable optical systems are increasing in many fields, which makes the limitations of traditional zoomable optical systems increasingly prominent. In this context, tuneable lens technology, which achieves no mechanical motion through physical field tuning, has emerged to provide a new solution for optical system optimisation.

Tuneable lenses achieve zoom by directly or indirectly altering the curvature or refractive index of the lens using electrical, thermal, or environmental stimuli. This process enables focus adjustment without mechanical movement, significantly simplifying the system structure [7]. Through the refractive index zoom lens, an applied electric field is used

to change the optical medium's arrangement to form a gradient refractive index distribution, commonly found in liquid crystal lenses [8,9]. Through variable curvature zoom lenses, the interior of the lens is mainly liquid or solid. The shape of the lens is directly or indirectly changed by the electric wetting effect [10], memory alloy actuator [11,12], piezoelectric actuator [13–15], or dielectric elastomer actuator (DEA), which directly or indirectly changes the shape of the lens to achieve zoom.

Dielectric elastomers (DEs) are flexible polymer materials (e.g., silicone rubber, acrylic elastomers) driven by the electric field-induced Maxwell stress effect. When an electric field is applied, the electrostatic pressure generated by the electrodeposition compresses the thickness and expands the area of the film, resulting in a large strain output. Dielectric elastomer-driven tuneable lenses (DETLs) have the advantages of fast response, light weight, vibration resistance, low power consumption, and high energy density and show great potential in optical systems [16,17].

Although tuneable lenses have been previously introduced in the review literature [7,18], this review mainly focuses on DETLs and systematically comprehends the recent advances, applications, and challenges in this field. This review not only analyses the driving principle and driving mechanism of DETL in detail but also focuses on the advantages and limitations of DETL with different structures and synthesises the research trends in materials, structures and optics. The full text is structured as follows: Chapter 2 classifies and analyses the zoom working principle of DETLs; Chapter 3 introduces the structural types of DETLs; Chapter 4 compares the performance of several classical DETLs; and Chapter 5 reviews innovative applications in areas such as auto-zoom imaging systems, micro-imaging, and augmented reality displays, while summarising the technical challenges facing DETL concerning materials, modelling and control, processes, and optical properties. Through this review, we aim to provide theoretical support and technical reference for the innovative research and development of DETL.

2. Principle of DETL

Currently, there are several ways to categorise DETL. With its rapid development, many classification methods cannot fully cover the types of lenses or adequately differentiate them individually. This paper classifies lenses according to their tuning principles and structures. Among them, the tuning principle is mainly divided into two categories: deformation-based and displacement-based zoom. The former achieves zoom by changing the lens shape through a dielectric elastomer actuator, while the latter accomplishes zoom by driving the axial or radial displacement of the lens position. The structure of the lens is divided into monolithic, composite, array, and metalenses, with a certain correspondence between them, as shown in Table 1.

Tuning Principle	uning Principle Subtype		Type of DEA	
Deformation-based	Direct Drive	Monolithic Lens Planar DEA, Spherical DEA and Con		
		Lens Array	Planar DEA	
	Indirect Drive	Monolithic Lens	Spherical DEA	
		Lens Array	Spherical DEA	
Displacement-based	Axial Displacement	Composite Lens Planar DEA and Bending-Mode		
	Lateral Displacement	Lens Array	Planar DEA	
		Metalens	Planar DEA	

Table 1. DETL classification (author's original classification).

Based on this categorisation, this chapter first introduces the working principle of DEA, followed by a detailed description of the principles and structures of various types of DETLs.

2.1. Principle of DE

The core principle of DE to realise the actuation function is mainly the electrostriction effect. When an electric field is applied to the ends of a DE, a series of complex changes occur in the internal microstructure of the material, leading to macroscopic deformation.

From a microscopic point of view, there are many polar groups in the molecular chain of DE. In the absence of an electric field, the orientation of these polar groups is randomly distributed. After applying the electric field, the electric field force will prompt the polar groups to rotate and rearrange so that the molecular chain is gradually oriented toward the electric field. This change in the orientation of the molecular chains will change the interaction force between the molecular chains, which will result in stretching or compression of the molecular chains. When the electric field strength is low, the orientation change of molecular chains is relatively orderly, and the deformation of the material is approximately linear with the electric field strength; with the increasing electric field strength, the orientation of molecular chains gradually tends to be saturated, and the growth rate of the deformation of the material is slowly slowed down, and at this time, the deformation of the material shows a nonlinear relationship with the electric field strength [19].

Macroscopically, the electrostriction effect is manifested as the DE shrinks in the thickness direction and expands in the plane direction. This is because under the action of the electric field, the Maxwell stress generated inside the material will compress the material, making it thinner in the thickness direction; according to the principle of conservation of volume of the material, the reduction in the thickness direction is inevitably accompanied by the expansion in the planar direction [20]. Figure 1 shows its driving principle diagram. When the DE is used as the driving element of the tuneable lenses, this expansion in the plane direction will affect the lens, which in turn changes the lens's focal length.

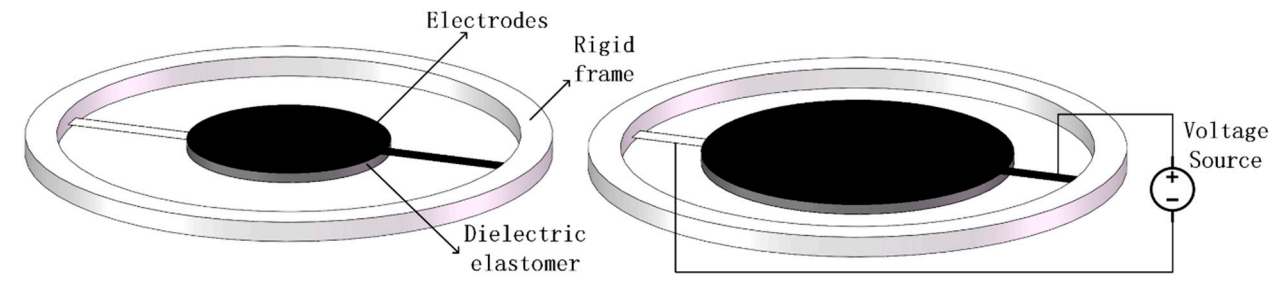


Figure 1. Principle of DE (author's original image).

Numerous factors affect the electrostriction effect, among which is the electric field strength, which is the most direct and critical factor. Generally speaking, the deformation of the material gradually increases as the electric field strength increases [21,22]. However, when the electric field strength exceeds the breakdown field strength of the material, electrical breakdown of the material is triggered [23]. DE materials have different breakdown field strengths, usually 10–100 MV/m [24]. In practice, the strength of the applied electric field must be strictly controlled to ensure that it is within the safe working range of the material. The frequency of the electric field also affects the electrostriction effect. Under a low-frequency electric field, the polar groups inside the material have enough time to respond to the change in electric field, and the electrostriction effect can be fully utilised; however, under a high-frequency electric field, the orientation of the polar groups cannot keep up with the rapid change in the electric field, which will lead to the weakening of the electrostriction effect. The response speed of the material will be limited [25].

Appl. Sci. 2025, 15, 6926 4 of 29

In addition, the material's properties, such as temperature, dielectric constant, and cross-linking density, also significantly affect the electrostriction effect. Increasing temperature intensifies the molecular thermal motion and reduces the material's elastic modulus, thus affecting the electrostriction effect [26]. Materials with higher dielectric constants can store more electrical energy at the same electric field strength, resulting in greater electrostriction [27]. The crosslink density determines how closely the molecular chains are connected, and an appropriate crosslink density can enhance the mechanical properties and stability of the material. Still, a crosslink density that is too high may restrict the movement of the molecular chains, thus weakening the electrostriction effect [28].

2.2. Tuning Principle

According to the tuning principle, DETL is mainly divided into two categories: (1) deformation-based driving, which involves directly or indirectly tuning the lens curvature to change the zoom using DEA; (2) displacement-based zoom, which uses DEA to drive the lens and produce axial or vertical axial displacement for zooming.

2.2.1. Deformation-Based

Methods based on deformation zoom mainly utilise DE driven by voltage to produce in-plane expansion. The radius of curvature of the spherical crown of the lens is directly or indirectly modulated to achieve zoom. The principle is shown in Equation (1):

$$\frac{1}{f} = (n-1)(\frac{1}{R_1} - \frac{1}{R_2}) \tag{1}$$

where R_1 and R_2 are the radii of curvature of the front and back spherical crowns, n is the refractive index of the lens, and f is the lens's focal length [29].

1. Direct drive

Tuneable lenses with direct actuated deformation are mainly used by DEA to change the shape of liquid or soft-solid lenses directly, enabling the dynamic change in focal length. Carpi et al. [30] developed a biconvex lens structure by combining a fluid-filled elastomer lens with a DEA, as shown in Figure 2a. The lens consists of two layers of pre-stretched transparent elastomer film forming a cavity, with the centre filled with transparent fluid and coated with flexible electrodes in an annular region around the lens. When a voltage is applied, the ring actuator generates an electrostatic compressive stress in the thickness direction, which triggers a radial contraction and directly drives the lens to produce a radial dimensional reduction. Since the fluid volume inside the lens is constant, its thickness increases, and the radius of curvature decreases. The lens has a magnification ratio of up to 129.1% and an operating frequency range of 1–10 Hz Pieroni et al. [31] developed a softsolid tuneable lens, as shown in Figure 2b, with a magnification ratio of up to 154.6%, by drawing on the regulation mechanism of animal lenses. Its preparation process is more concise and efficient than liquid lenses. The lens designed by Son et al. [32] achieves the zoom function by deforming the film to create a bump or depression, with a magnification ratio of 124% and a frequency response of up to 20 Hz.

Direct-drive anamorphic tuneable lenses feature a compact structure and small size, thanks to the high level of integration between the driver and the lens. This integration provides a significant advantage in portable devices and space-constrained application scenarios. Moreover, direct-drive solutions generally exhibit a faster response time and simpler control, making them ideal for systems with demanding dynamic performance requirements. However, the volume and deformation capacity of the driver limit the direct drive method, resulting in a relatively small focal length adjustment range that makes it challenging to accommodate a wide array of zoom requirements.

Appl. Sci. **2025**, 15, 6926 5 of 29

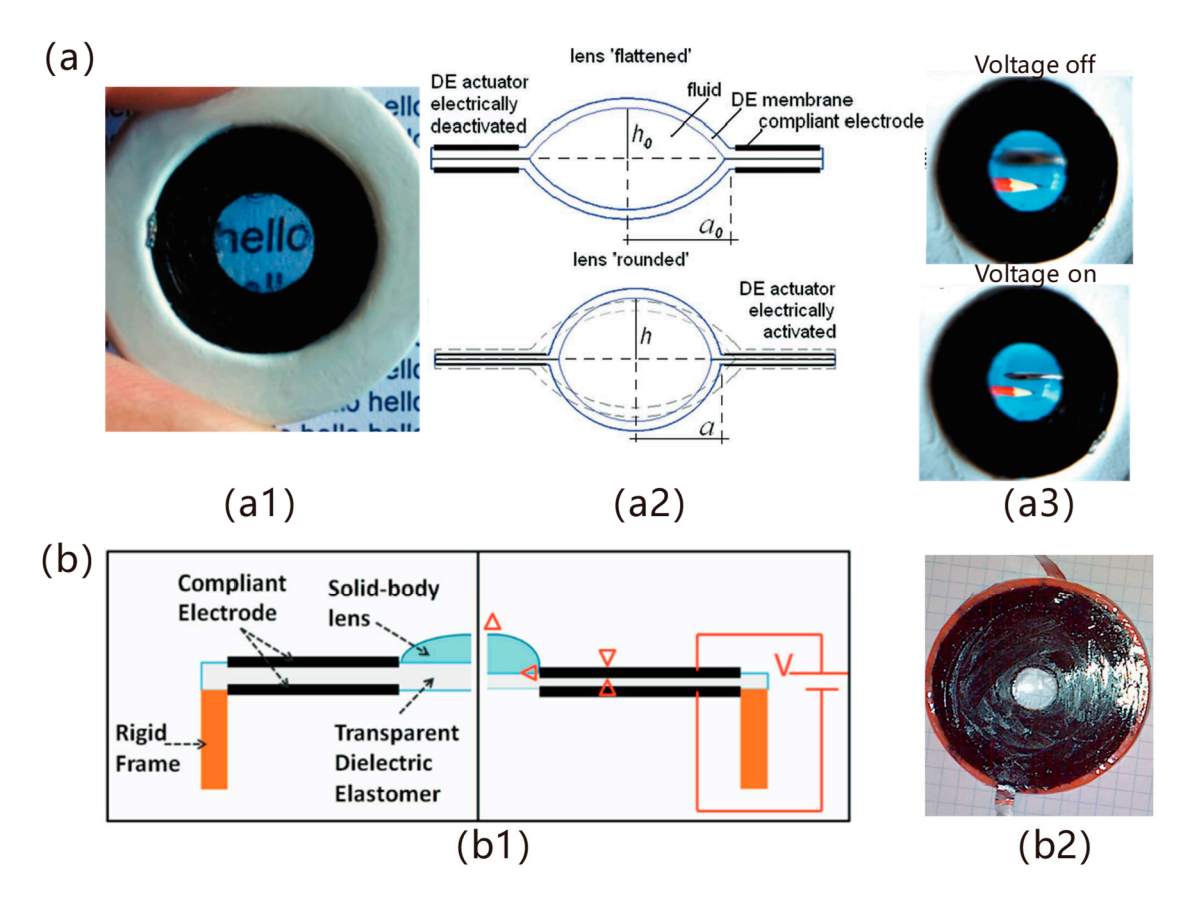


Figure 2. Directly driven deformable DETL. (a) Direct deformation liquid lens: (a1) lens physical top view; (a2) lens zoom principle diagram, the upper picture is the shape of the lens when no voltage is applied, and the lower picture is the DEA squeezing the lens after applying a voltage to make the shape change; (a3) lens zoom imaging effect diagram [30]. (b) Direct deformation soft solid lens: (b1) lens zoom principle diagram, where the left side shows the shape of the lens when no voltage is applied, and the right side shows the soft solid lens squeezed by DEA after applying voltage, which makes the shape change; (b2) top view of the lens in kind [31].

2. Indirect drive

Compared to direct-drive DETL, indirectly driven zoom lenses are typically configured with a liquid chamber connected to the outside. The DEA induces deformation of the passive film (e.g., polydimethylsiloxane (PDMS) elastomer film) by compressing the liquid medium inside the chamber, thereby achieving the indirect tuning of the lens curvature. Lau et al. [33] constructed a diaphragm-pump-type adjustable liquid lens driven by the DEA, as shown in Figure 3, which can change the focal length through the DEA by adjusting the hydraulic pressure of the diaphragm pump; the lens is filled and discharged to change the focal length, and its magnification ratio can be up to 333%. Zhang et al. [34] proposed a hydrogel electrode-coupled tuneable lens structure. They carried out the corresponding theoretical analyses, which utilised the deformation generated by the DEA to change the volume of the other cavity, which provided a new idea for the tuneable lens. Wei et al. [35] developed a concentric annular dielectric elastomer-driven liquid lens; this lens's circular and annular cavities are interconnected and filled with liquid. The degree of bending of the lens membrane is adjusted indirectly by applying a voltage to change the volume of liquid in the annular region to achieve the zoom function; the experimental results show that the zoom ratio of this lens can be as high as 414%, and it has a better imaging quality. Cheng et al. conducted a detailed theoretical analysis and experimental verification of the configuration and explored the main factors affecting the focal length of the liquid lens through theoretical analysis [36]. Shi et al. added a detailed theoretical analAppl. Sci. **2025**, 15, 6926 6 of 29

ysis of the variation range of the focal length of the configuration based on pre-stretching, which provided a thorough theoretical basis for the optimal design of the lens [37].

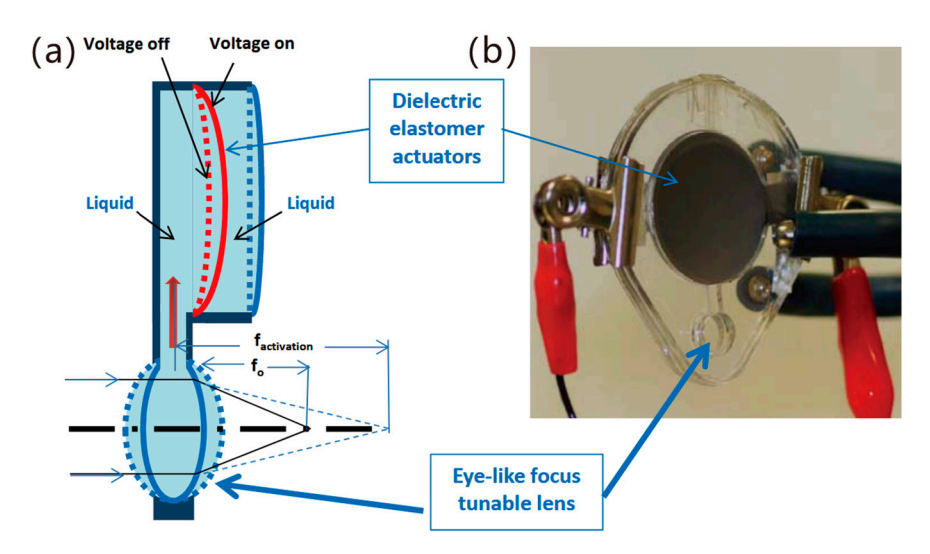


Figure 3. Indirectly driven deformable DETL: (a) lens zoom schematic, the dotted line is the shape of the DEA and lens without voltage applied, and the realisation is the shape of the DEA and lens after the voltage is applied; (b) physical diagram of the lens [33].

Indirectly driven DETLs transmit deformation forces through a liquid, enabling a wider zoom range and making them more suitable for application scenarios that require significant focal length adjustments. However, such lenses typically rely on a liquid or gas cavity connected to the outside, often several times the size of the lens body, increasing the overall system's size and complexity. Additionally, the preparation process is more complicated, potentially affecting the reliability and lifespan of the system.

2.2.2. Displacement-Based

In contrast to deformation-based lenses, displacement zoom lenses primarily employ DEA to actuate the lens group, creating axial or vertical axial displacement to alter the focal length.

1. Axial displacement

The researchers employed DE as the primary component to address the drawbacks of the mechanical displacement zoom system, which is considerable in size and weight. They realised flexible drive zoom by mechanically connecting the DEA to either a solid or soft-solid lens. When an electric field is applied to the dielectric elastomer, the elastomer contracts and moves the lens along the optical axis, thereby altering the distance between the lens and the object or imaging plane to achieve the zoom effect. This principle mirrors the focus adjustment method found in traditional optical systems, and its specific expression is illustrated in Equation (2) [29]:

$$\frac{1}{u} + \frac{1}{v} = \frac{1}{f} \tag{2}$$

where u is the object distance, v is the image distance, and f is the focal length.

Kim et al. [38] fabricated three different structures of DEA-driven micro-optics, where an applied voltage can cause the DEA to produce displacement in the direction of the extended optical axis to achieve zoom. Yun et al. [39] developed a displacement lens via DEA with the structure shown in Figure 4a, which consists of a convex hemispherical PDMS lens and a DEA. By applying a voltage, the deformation of the DE film enables the lens

Appl. Sci. **2025**, 15, 6926 7 of 29

to change in the vertical direction and thus change the focal length, with a magnification ratio of up to 118.4%, a displacement attenuation of less than 9% for 250,000 consecutive cycles of operation, and good durability.

The DETL, which shifts the zoom along the optical axis, has effectively achieved miniaturisation compared to conventional shift-type lenses. However, compared to the variable-form DETL, it has a larger zoom ratio and a greater axial dimension thickness.

Lateral displacement

Jin et al. [40] first developed a DETL with displacement zoom in the vertical optical axis direction, as shown in Figure 4b, which DE can drive to enable reciprocal motion in the vertical direction along the optical axis. A focal length change can be realised with another solid lens, but continuous zooming is impossible. On the other hand, tuneable lenses based on the principle of Fresnel and Alvarez lenses can achieve the constant zoom function by displacement in the vertical optical axis direction.

On the other hand, tuneable lenses based on the principles of Fresnel and Alvarez lenses achieve a continuous zoom function by displacing in the direction of the perpendicular optical axis while further enhancing the zoom capability.

Fresnel lenses satisfy the radius a of the Nth ring band by splitting the continuous surface of a conventional spherical lens into a thin sheet of concentric rings:

$$R_N^2 = NR_1^2 \quad (N = 1, 2, 3, ...)$$
 (3)

where R_1 is the radius of the first annular band. Each ring is an optical surface with a specific curvature, and these rings are designed so that the lens as a whole still has refractive power, but reduces the thickness and weight of the lens. By varying the spacing of the rings, the Fresnel lens allows for focal length adjustment [41]. The initial focal length F is related to the wavelength λ and the radius of the ring band as:

$$F = \frac{R_1^2}{\lambda} = \frac{R_N^2}{N\lambda} \tag{4}$$

When the radius of the ring band shrinks due to deformation to S times the original radius $(S = R'_N/R_N)$, the new focal length F' is

$$F' = S^2 F \tag{5}$$

Based on this principle, Park et al. [42] developed a dielectric elastomer-driven Fresnel lens with the structure shown in Figure 4c. The device structure comprises a binary phase Fresnel zone plate, a ring-shaped deformable electrode, and a DE membrane. By regulating the radius of the zone plate by DEA, the Fresnel lens can achieve a zoom function with a magnification ratio of up to 109.1% and a response speed of up to 23 ms.

An Alvarez lens usually combines two curved lenses with different optical properties, whose curvature and thickness can be flexibly adjusted to form specific optical properties. The lateral displacement of the lens elements can change optical properties such as focal length and field of view [43]. The following cubic polynomial describes the free surface thickness distribution of a single Alvarez lens element:

$$t = A\left(xy^2 + \frac{x^3}{3}\right) + Dx + E \tag{6}$$

where A is the depth of the control free surface modulation, D is the tilt coefficient, E is the voxel thickness added to the cubic surface equation at the centre, t is the phase distribution of the Alvarez lens, and x, y are the transverse and longitudinal coordinates. When the

Appl. Sci. 2025, 15, 6926 8 of 29

DEA drives the two phase plates to produce a relative transverse displacement δ , the focal length f of the system is

 $f = \frac{1}{4\delta A(n-1)} \tag{7}$

where δ represents the lateral displacement, and n denotes the refractive index of the lens material [44].

Chen et al. [45] used this principle to develop a dielectric elastomer-driven Alvarez lens based on DE, as shown in Figure 4d. The lens consists of multiple Alvarez lens elements and a DE film.

Alvarez lenses based on dielectric elastomer actuation provide an innovative solution for high-performance DETL. By designing the phase plate, not only can a wide range of continuous zoom be realised, but also the field of view can be changed. However, this also challenges the preparation process and focal length control. The precision processing of the phase plate is related to the imaging quality of the lens, and the control accuracy is associated with the precise lens tuning.

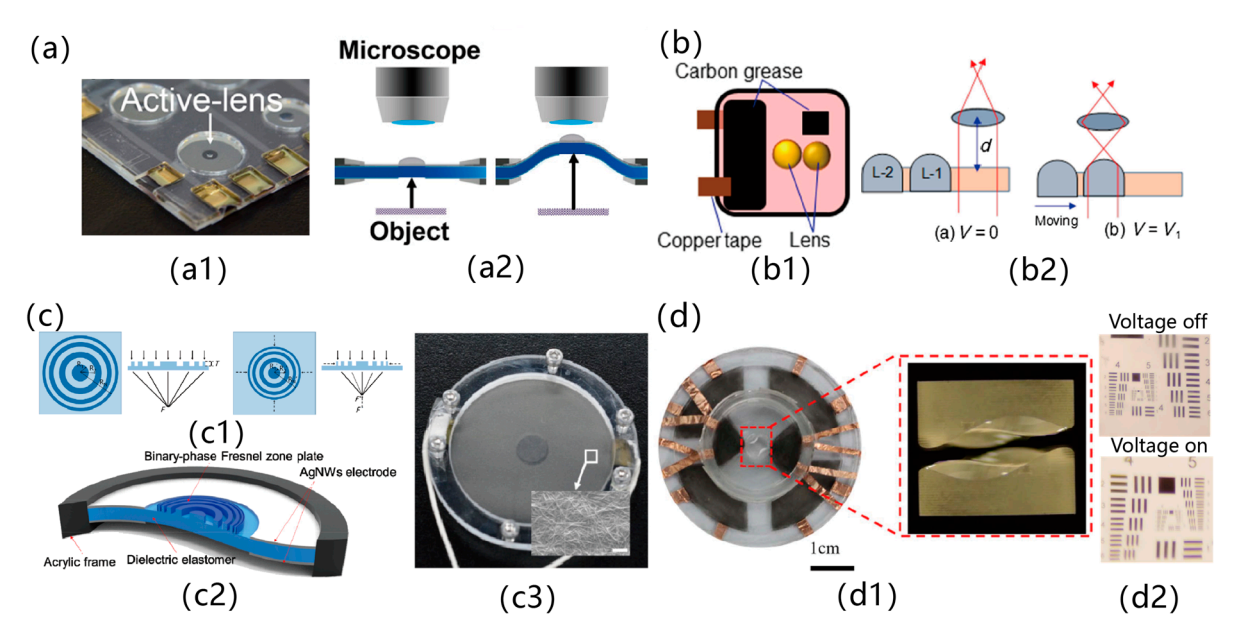


Figure 4. Displacement-based DETL. (a) Displacement in the optical axis direction: (a1) Physical diagram of the lens; (a2) schematic diagram of the lens zoom, where the left figure shows the initial state of the lens without applying a voltage, and the right figure shows the displacement of the lens along the optical axis direction after applying a voltage, which makes the focal length change [39]. (b) Displacement in the vertical optical axis direction: (b1) schematic diagram of the structure of the lens; (b2) schematic diagram of the lens zoom, where the left figure shows the lens without applying a voltage in the initial state, and the right figure shows that for the applied voltage after the lens L-1 is perpendicular to the direction of the optical axis displacement, so that the focal length changes [40]. (c) Alvarez lens: (c1) lens zoom schematic, the left figure for the initial state of the lens without the application of the voltage, the right figure for the application of the voltage after the DEA drive concentric ring radius change, so that the focal length changes; (c2) schematic diagram of the structure of the lens; (c3) top view of the lens in kind [42]. (d) Fresnel lens: (d1) top view of the Alvarez lens; (d2) zoom effect of the lens; the top and bottom pictures are the imaging pictures before and after, respectively [45].

3. Lens Construction

According to the structure, DETL is mainly classified into (1) monolithic lenses—lenses coupled with planar, spherical, or conical DEA; (2) composite lenses—sets of lenses combined with annular or curved DEA; (3) arrayed lenses—miniature lens units forming

arrays that the DEA drive; and (4) metalenses—super-surface structures generated on the DEA and tuned by the DEAs.

3.1. Monolithic Lens

Monolithic lenses facilitate compact and efficient optical tuning by connecting a dielectric elastomer driver to the lens. Ordinary monolithic tuneable lenses are classified into three types based on planar, spherical, and conical DEA drivers according to the type of DEA.

1. Planar DEA

The three primary forms of planar actuators are ring, disc, and sector. These actuators are essential in tuneable lens design due to their mature manufacturing process and easy integration. According to the structure, planar actuator-driven DETLs are mainly nonconvex, biconvex, and droplet lenses.

Kim et al. [46] were the first to propose an annular DEA to drive a monoconvex silicone lens (Figure 5a), verifying this configuration's feasibility to achieve zoom. Nam et al. [47] used a disc-shaped driver through structural optimisation to achieve lens zoom with the help of an internal frame fixation and an external fan-coupler driver, as shown in Figure 5b. They achieved a zoom ratio of 165.7% at a driving voltage of 5 kV. Chen et al. [48] prepared a monoconvex ion eye using ion gel as both lens and electrode materials, as shown in Figure 5c. A disc-type DEA was sandwiched between the lens and electrode, and the deformation of the DEA after the voltage application drove the lens's deformation to achieve the zoom. The zoom ratio could reach ~150%. Ghilardi et al. [49] innovated to divide the electrode into four sectors, as shown in Figure 5d, and induced lens deformation by asymmetric driving to achieve active regulation of aberration, which provides ideas for improving imaging quality.

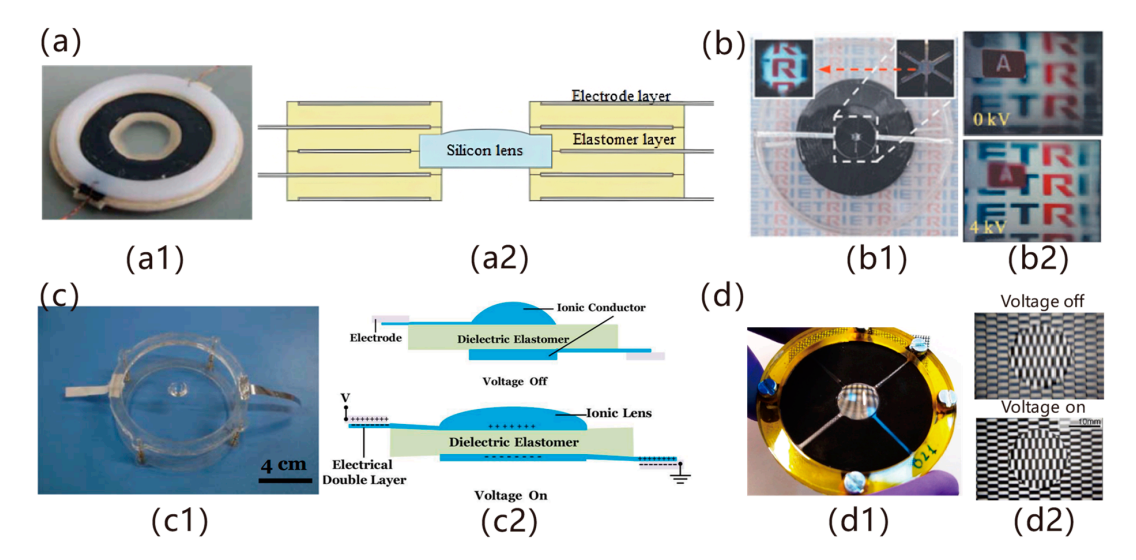


Figure 5. Planar actuator-driven monoconvex DETL. (a) Driven based on a butyl rubber DEA: (a1) top view of the lens object; (a2) schematic diagram of the lens structure [46]. (b) Driven using a sector coupler: (b1) top view of the lens object; (b2) lens zooming effect, the upper and lower figures show the imaging effect before and after applying the voltage, respectively [47]. (c) Solid-state lens driven by a disc-type DEA: (c1) top view of the lens object; (c2) lens zoom schematic, the upper and lower diagrams show the shape of the lens before and after the application of voltage, respectively, '+' and '-' indicate positive and negative charges respectively [48]. (d) Adjustable aberration lens driven by a sector-type DEA: (d1) top view of the lens object; (d2) lens aberration regulation effect, the upper and lower diagrams show the imaging effect of the lens before and after the application of voltage, respectively [49].

Biconvex lenses have attracted much attention in the field of bionic optics due to their resemblance to the human eye lens, and Carpi et al. [30] first proposed an 'electronic eye'

design that combines an adjustable corneal lens with a bionic lens. Maffli et al. [50] designed a biconvex liquid lens driven by a circular silicone rubber dielectric elastomer, as shown in Figure 6a. This lens features a magnification ratio exceeding 120% and a response time under 175 microseconds, which is the fastest DETL in terms of response time currently available. Wang et al. [51] developed an all-solid-state adjustable soft lens, as shown in Figure 6b, with a focus variation range of up to 209%. For the performance enhancement of biconvex lenses, Lu et al. [52] performed a detailed theoretical analysis based on ring driver-driven biconvex liquid lenses, explored the influence of multiple parameters on the lens performance, and solved the coupling and non-uniform deformation problems of deformable lenses. Wang et al. [53] proposed a concise computational model based on the assumption of uniform deformation, applying the energy method, and matched well with the realisation results. Liu et al. [54] used 3D printing technology to print transparent conductive gels as lenses on both sides of DE to prepare a biconvex solid lens, as shown in Figure 6c. When a voltage is applied to the lens, its intermediate disc-type DEA produces deformation to drive the lens deformation to achieve zoom, and its zoom ratio can reach a maximum of 181%, with a shortest response time of up to 80 ms.

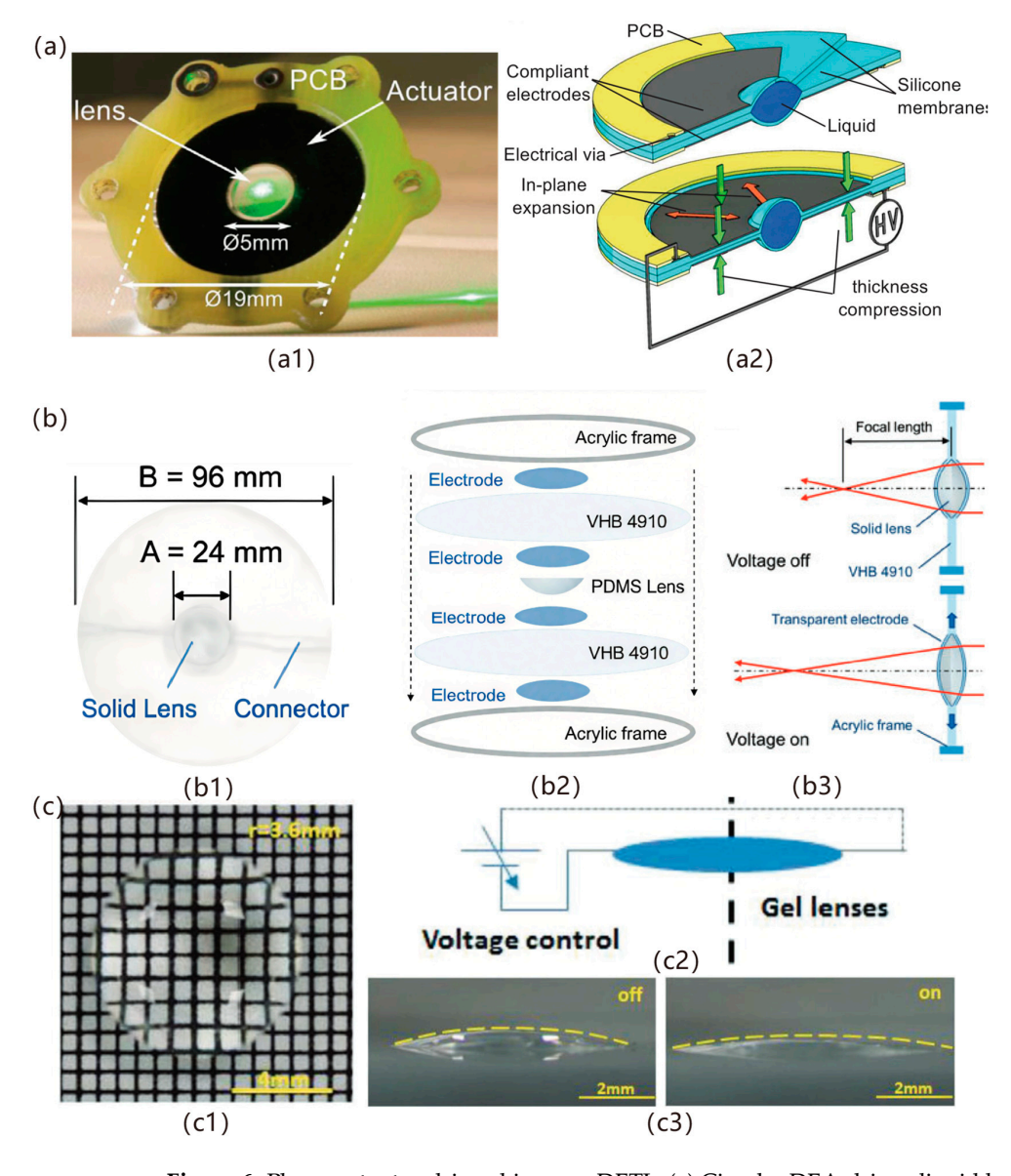


Figure 6. Planar actuator-driven biconvex DETL. (a) Circular DEA-driven liquid lens: (a1) lens physical diagram; (a2) lens structure and zoom principle schematic diagram; the upper and lower diagrams,

respectively, show the effect before and after applying voltage to the lens [50]. (b) Circular DEA-driven solid lens: (b1) lens physical top view; (b2) lens structure schematic diagram; (b3) lens zoom. The schematic diagram of the principle, as well as the upper and lower diagrams, shows the focal length change after applying voltage to the lens, respectively [51]. (c) Disc-shaped DEA-driven solid lens: (c1) top view of the lens object; (c2) schematic diagram of the lens driving principle; (c3) diagram of the lens morphology change, where the left and right diagrams show the side view of the lens morphology before and after applying voltage, respectively [54].

The core principle of dielectric elastomer-driven droplet lenses is to fill liquid droplets on the surface of small pores or hydrophobic layers, creating biconvex or monoconvex surfaces through the liquid's surface tension. When a voltage is applied to the DE to deform it, the droplet curvature changes with the deformation of the DEA. Jin et al. [55] prepared two small droplet lenses with different scales by filling glycerol droplets into the holes of a DE film, as shown in Figure 7a. After applying a voltage, the lens's aperture decreases, thereby causing the lens's focal length to change. This lens has a zoom ratio of up to 140%, but it is significantly affected by gravity, and the gravity effect needs to be suppressed by reducing the lens size. Huang et al. [56] prepared a droplet lens by placing a glycerol-sodium chloride mixture droplet into the middle of an annular hydrophobic layer, and the droplet curvature control was realised by modulating the infiltration region with an electric field. Cheng et al. [57,58] designed two different droplet prehensile ratio lenses, as shown in Figure 7b, and the zoom ratio reached up to 252% through a disc-type DEA.

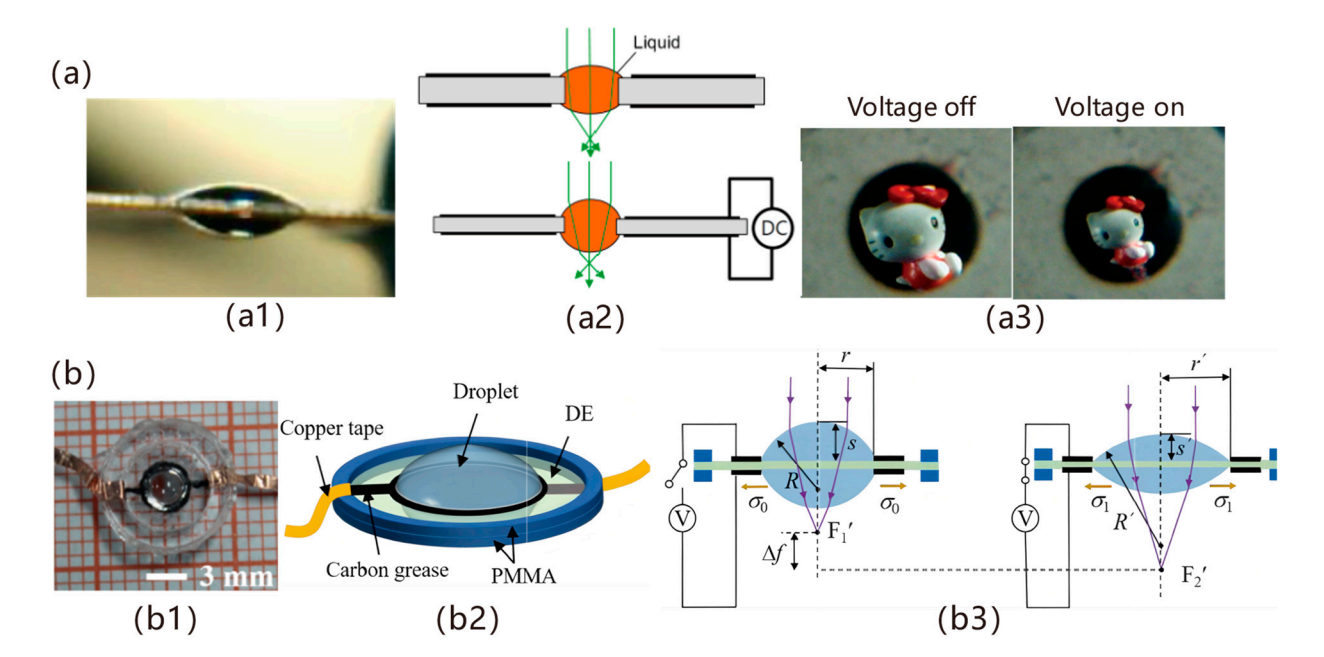


Figure 7. Planar actuator-driven droplet DETL. (a) Annular DEA-driven biconvex lens: (a1) top view of the lens object; (a2) schematic diagram of the lens zoom principle, the upper and lower diagrams show the focal length change of the lens before and after the application of the voltage, respectively; (a3) diagram of the lens zoom effect, the left and the right diagrams are the lens imaging images before and after the application of the voltage, respectively [55]. (b) Disc-shaped DEA-driven biconvex lens: (b1) top view of the lens object; (b2) schematic diagram of the lens structure; (b3) schematic diagram of the lens zoom principle; the left and right figures show the focal length change of the lens before and after applying the voltage, respectively [58].

In planar DEA-driven DETL, the lenses are made of monoconvex soft solids like silicone rubber, which offer excellent impact resistance and a simpler preparation process. However, compared to biconvex lenses, they have a smaller field of view and poorer im-

age quality. Biconvex lenses, on the other hand, use soft solids or liquids as lens materials, resulting in superior imaging quality. Moreover, substituting the material of the biconvex lens with a conductive substance (e.g., NaCl solution or conductive gel) can further simplify its preparation process and reduce lens power. The droplet lens is easy to prepare due to its non-encapsulated structure, and the protruding droplets formed under surface tension possess a uniform spherical crown shape. In comparison to encapsulated lenses, droplet lenses typically provide higher imaging quality. However, droplet lenses face limitations in size, and their application in complex environments, such as vibration, is also restricted.

2. Spherical DEA

Spherical dielectric elastomer-driven DETLs are driven by hemispherical or spherical DEAs that match the shape of the lens surface. Hemispherical DEAs typically use electrode materials with excellent light transmission, and zoom is achieved by varying the pressure inside the cavity when a voltage is applied. In contrast, spherical DEAs do not have electrodes coated in the centre of the light-through aperture, and zoom is achieved by adjusting the curvature of the light-through region of the lens when a voltage is applied.

Liang et al. [59] developed a DETL, shown in Figure 8a. It comprises a bent PDMS film sandwiched between a gold electrode and a sodium chloride solution. Upon voltage application, the film area expands, causing the central region to bulge, changing the lens's focal length. The magnification ratio can reach 122.9% at 900 V driving voltage.

Dual-cavity lenses achieve a wide range of zoom through pressure changes. Shian et al. [60] proposed a dual-cavity lens configuration, as shown in Figure 8b, consisting mainly of two liquid cavities with a transparent DEA sandwiched between them. In the initial state, the liquid pressure inside the two liquid cavities differs, making the two projections have different curvatures. After applying a voltage, the driver membrane will deform, thus changing the pressure distribution inside the liquid cavities and causing the lens's focal length to change. The lens can reach 400% of the variation ratio, and the response speed is tens of milliseconds. Yang et al. [61,62] optimised the chamber parameters to achieve a rise time of 75 ms at 154.81% of the variation ratio. Zhang et al. [63] established a computational model based on the structure. Theoretically, they analysed the effects of the chamber radius, shear modulus, permittivity, pre-stretching ratio, and the injected liquid's volume on the lenses' tuning performance. Parameters on the lens's tuning performance show that liquid volume adjustment can achieve positive and negative focal length switching, expanding the tuning dimension.

Shian et al. [64] proposed an active–passive membrane structure, as shown in Figure 8c, in which the lens consists of upper and lower acrylic DE membranes: one layer adopts VHB 4905, which has been pre-stretched by 100%, as the passive membrane, and the other layer adopts VHB 4910, which has been pre-stretched by 300%, as the active driving membrane. When a voltage was applied to the active membrane, a synergistic change in the curvature of the active and passive membranes was triggered, and the magnification ratio was up to 203%. Cao et al. [65] developed a lens parameter-focus mapping model based on this configuration. Li et al. [66] prepared a spherical deficient DEA-driven focusable lens, as shown in Figure 8d, with a magnification ratio of up to 132.6%. The team then conducted detailed modelling of hemispherical and ball-deficient-shaped active–passive membrane structure lenses. It analysed the effects of different parameters on the lens performance, which enriched the theoretical basis for its structural design [67].

Spherical DEA-driven DETL features a more compact structure for the same light-through aperture. However, its response may take longer after applying voltage due to the liquid pressure under initial conditions. Additionally, there could be a liquid leakage issue during its preparation, which affects the lens's stability.

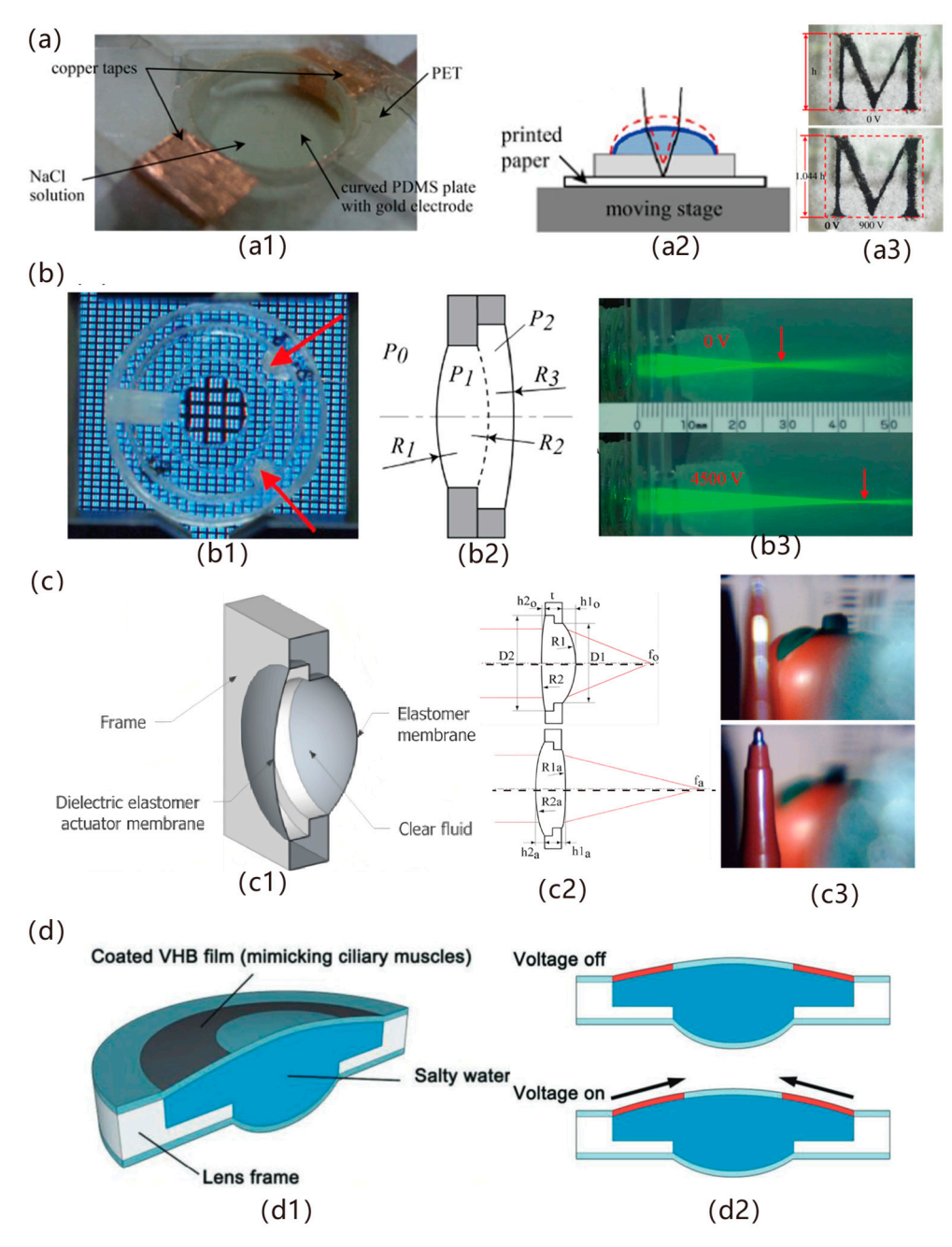


Figure 8. Spherical actuator-driven DETL. (a) Hemispherical DEA-driven liquid single-cavity lens: (a1) top view of the lens object; (a2) lens zoom schematic, the solid and dashed lines are the shapes of the lens before and after the application of the voltage, respectively; (a3) lens zoom effect diagram, the upper and lower diagrams are the imaging images of the lens before and after the application of the voltage, respectively [59]. (b) Hemispherical DEA-driven liquid double-cavity lens: (b1) top view of the lens object; (b2) schematic diagram of the lens structure; (b3) lens zoom effect diagram, the upper and lower diagrams, respectively, before and after the application of the voltage, the focal position changes after the laser passes through the lens [60]. (c) Hemispherical DEA-driven active—passive membrane structure: (c1) schematic diagram of the lens structure; (c2) lens zoom schematic diagram, the upper and lower diagrams, respectively, before and after the application of the voltage, the focal position changes; (c3) lens zoom effect diagram, the upper and lower diagrams are the imaging pictures of the lens before and after the voltage change, respectively [64]. (d) Spherical DEA-driven active—passive membrane structure (d1) schematic diagram of the lens structure; (d2) lens zoom principle diagram [66].

3. Tapered DEA

Hu et al. [68] developed a conical dielectric elastomer-driven tuneable lens, shown in Figure 9a, which achieves zoom by squeezing the intermediate PDMS deformer with a conical DEA. The focal length was at a minimum when no voltage was applied, and the axial squeezing force on the deformer decreased after the voltage was applied, leading to an increase in the focal length and a zoom ratio of up to 178.2%. Yin et al. [69] introduced a self-recovering paper folding mechanism (Figure 9b), which achieves a zoom ratio of 117% at a driving voltage of 3.5 kV using the axial-radial force conversion mechanism of the tapered DEA.

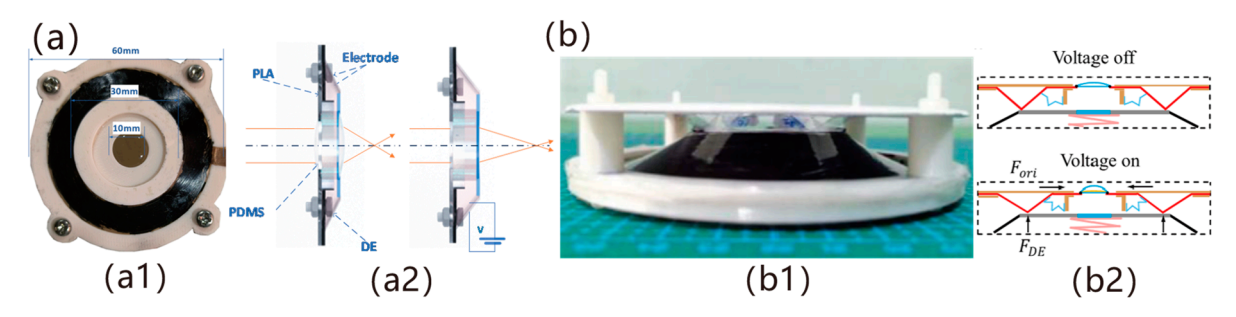


Figure 9. DETL driven by a conical actuator. (a) All-solid lens: (a1) top view of the lens object; (a2) lens zoom schematic diagram, the left and right diagrams show the change of focal length before and after the application of voltage, respectively [68]; (b) origami structure lens: (b1) side view of the lens object; (b2) lens zoom schematic diagram, and the upper and lower diagrams show the change in lens shape before and after the application of voltage, respectively [69].

The DETLs based on a conical DEA drive with a predominantly soft solid lens demonstrate better stability. Additionally, they may exhibit a faster response time due to the force exerted on the DEA by the soft solids or springs in the initial conditions. However, the lenses associated with this configuration are susceptible to errors during the preparation process, which makes them more prone to aberrations during the operation process.

3.2. Composite Lenses

Composite lenses primarily drive hard or soft solid lens sets through DEA for zoom. Yun et al. [70] developed a bi-directionally driven zoom module, as shown in Figure 10a, which consists of two parallel-connected movable lenses, one with a convex lens structure and the other with a concave lens structure. Each movable lens is subjected to the deformation of the film and electrostatic attraction to generate a bidirectional translational motion to achieve zoom. It has the advantages of fast response, high repeatability, and low power consumption. Pu et al. [71] developed a DEA based on a single-layer nanocomposite material for long travel displacements, and its structural design is shown in Figure 10b. The device employs six DE units with symmetrical distribution to form a disc-shaped actuator. The electrically induced deformation drives the lens to adjust the displacement in the direction of the optical axis. It is used with the fixed-focus optics set to construct an efficient miniaturised zoom system. The lens can generate a maximum bi-directional linear displacement of ±1.38 mm at a driving voltage of 1000 V, and its dynamic response is characterised by a driving response time of 330 ms and a fast reset time of 100 ms. Meanwhile, the zoom system maintained 97.5% of the initial displacement after 10,000 cycles of continuous operation without significant material fatigue or dielectric degradation.

Composite DETLs, offering a greater zoom range than monobloc DETLs, are generally more complex in their construction.

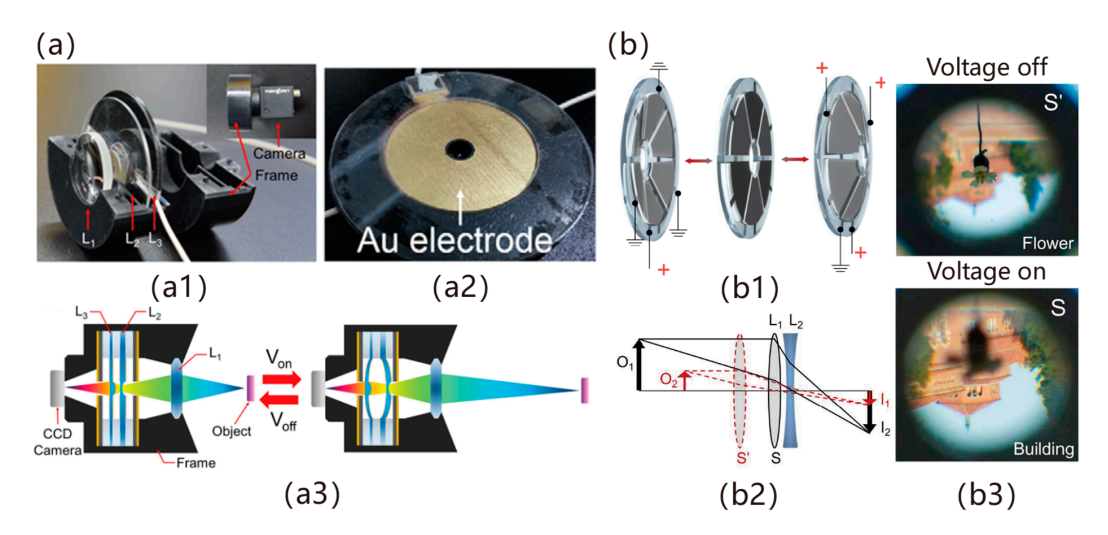


Figure 10. Composite DETL. (a) PDMS lens: (a1) physical diagram of the zoom system; (a2) top view of the lens in kind; (a3) lens zoom schematic diagram; the left and right diagrams are the change in focal length before and after applying the voltage, respectively [70]. (b) Curved DEA drive: (b1) lens displacement along the optical axis direction schematic diagram; (b2) lens zoom schematic diagram, the solid and dotted lines are the change in focal length before and after applying the voltage, respectively; (b3) lens zoom effect diagram, the upper and lower diagrams are the imaging pictures of the lens before and after applying the voltage, respectively. voltage; (b3) lens zoom effect diagram, the upper and lower diagrams show the imaging pictures of the lens before and after applying voltage, respectively [71].

3.3. Lenes Array

Researchers propose the array lens to enhance the zoom range and imaging quality of DETL. As a new type of optical element, it comprises multiple small lenses, whose shape, position, or curvature can be adjusted to modify the focal length. Niklaus et al. [72] developed PDMS lens arrays, where the driver is bonded by sockets providing fluidic coupling, and the compressive deformation is achieved with the help of electrostatic force generated by an applied voltage to change the curvature of the lenses with a zoom ratio of up to 150%, withstanding millions of cycles. Wang et al. [73] developed a tuneable microlens array based on DE actuation, as shown in Figure 11a, where DEA drives the shape deformation of the lens array to realise the adjustment of lens curvature. The focal length of this lens can be adjusted from 950 mm to infinity with good imaging quality, which is suitable for machine vision systems, etc. Chen et al. [74] proposed a bionic compound eye imaging system, as shown in Figure 11b, which achieves a continuous optical zoom from $0.30 \times$ to $0.90 \times$ through the focal length linkage mechanism of the Alvarez lens array and the dual auxiliary lenses with a 50 lp/mm imaging resolution.

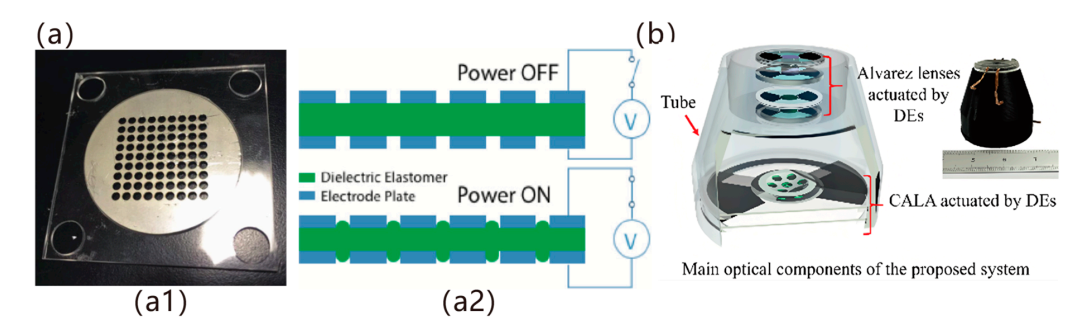


Figure 11. DEA-driven array DETL. (a) Planar array: (a1) top view of the lens object; (a2) lens zoom schematic, the upper and lower diagrams are the changes in the shape of the lens before and after the application of voltage, respectively [73]. (b) Curved array, where the left and right diagrams are the schematic and the object of the lens, respectively [74].

Array DETLs offer improved zoom range and imaging quality; however, their preparation process and imaging algorithm are more complex, which may impact the system's response time.

3.4. Metalenses

Wang et al. [75] first proposed constructing a two-dimensional gradient photonic crystal by embedding an array of DE tubes in an air background and adjusting the radius of the DE tubes by applying different voltages to change the filling factor of the two-dimensional gradient photonic crystal, which in turn adjusts the photon dispersion relation and the effective refractive index and achieves the focal length and field of view adjustment. With the development of technology, the theory gradually developed into hyperlens technology [76]. She et al. [77] developed a hyperlens based on DE actuation, as shown in Figure 12, which can simultaneously adjust the focal length, aberration, and image shift by DEA actuation and has a magnification ratio of 207%, which demonstrates an excellent potential for microscopy and compact optical systems.

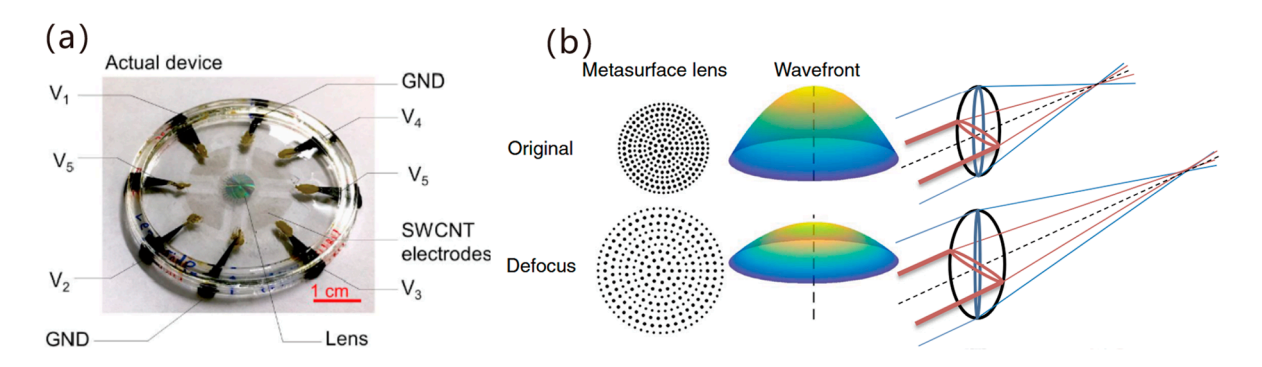


Figure 12. Dielectric elastomer-driven metalenses: (a) top view of the lens object; (b) schematic diagram of lens zoom, where the upper and lower diagrams show the change in focal length before and after applying voltage, respectively [77].

The emergence of dielectric elastomer-driven metalenses significantly reduces lens thickness and paves the way for innovative high-performance DETLs. However, compared to other DETL structures, its preparation process is more complex and demands more precise and coordinated control of focal length, aberration, and image quality offset.

4. Performance Comparison

There are some differences in the performance of DETLs with different tuning methods and structures. The primary liquid lens parameters reported publicly are listed and compared, which is of some reference significance for readers. The parameters compared in this review include tuning principle, lens structure, dielectric field strength, focusing ability, response time, DEA material, and other key indices. Among them, the dielectric field strength refers to the maximum electric field strength that the lens can withstand before breakdown; the focusing capability describes the physical range or the zoom ratio (the ratio of the maximum focus to the minimum focus) that the lens system achieves for the focus adjustment. Response time is then defined as the drive time required for the focal length to reach 90% of the change in focal length from voltage application when a square wave drive voltage is applied and the recovery time required to achieve 90% of the change in focal length after the voltage is withdrawn. The specific parameters are detailed in Table 2.

Appl. Sci. 2025, 15, 6926 17 of 29

Table 2. Comparison of DETL performance ('-' indicates unknown).

Year	Tuning Principle	Construction	Dielectric Field Strength	Focusing Ability	Response Time	DE Material	Ref.
2011 2011 2012 2013	Deformation-based Deformation-based Deformation-based Deformation-based	Monolithic Monolithic Monolithic Monolithic	150 V/μm 58 V/μm 25 V/μm 40 V/μm	16.72–22.73 mm 12.5–15.5 cm	60 ms - -	Nitrile rubber Acrylic (VHB 4905) Silicone (R-2652) Silicone	[46] [30] [32] [78]
2013	Deformation-based	Monolithic	45 V/μm	16 cm-770 cm	<1 s	Acrylic (VHB 4905, VHB 4910)	[64]
2014	Deformation-based	Monolithic	13.3 V/μm	25.4–105.2 mm	<450 ms (drive) <700 ms (recover)	Silicone (TC-5005 A/B)	[35]
2014	Deformation-based	Monolithic	36 V/μm	13.1–16.1 mm	-	Silicone (Sylgard 184)	[59]
2015	Deformation-based	Monolithic	-	Aperture 1.85 mm: 3–5.6 mm Aperture 0.376 mm: 400–620µm	540 ms (drive) 240 ms (recover)	Silicone (Daeil Material Compound, Trigonox 101-45S-ps)	[79]
2016	Displacement-based	Composite	17.5 V/μm	1.8–7.8 mm	<1 ms	Silicone (Elastosil P7670)	[70]
2017	Deformation-based	Array	5 V/μm	950 mm-∞	- <u>-</u>	Acrylic (VHB 4910)	[73]
2017	Displacement-based	Monolithic	$200\;V/\mu m$	15.4–20 cm	23 ms (drive) 93 ms (recover)	Silicone (Elastosil P7670)	[42]
2018	Displacement-based	Metalenses	-	50–103.5 mm	-	Acrylic (VHB 4905)	[77]
2019	Deformation-based	Monolithic	$44.1\;V/\mu m$	Zoom ratio: 180%	-	Acrylic (VHB 4910)	[65]
2020	Deformation-based	Monolithic	25 V/μm	4.32–8.35 mm	7.1 ms	Silicone (PDMS-MVS, PDMS-MOS)	[80]
2021	Deformation-based	Monolithic	41 V/μm	26.1–33.6 mm	-	Silicone (LSR 4305, 3 wt% CuPc)	[81]
2022	Displacement-based	Composite	24 V/μm	20–850 mm	330 ms (drive) 100 ms (recover)	Unimorph nanocomposite dielectric elastomer	[71]
2023	Displacement-based	Composite	71.4 V/μm	5.2–19.5 mm	124 ms (drive) 203 ms (recover)	Acrylic (VHB 4905)	[82]
2024	Displacement-based	Composite	33.6 V/μm	6.3~12.0 mm	150 ms (drive) 210 ms (recover)	Acrylic (VHB 4905)	[83]
2025	Displacement-based	Composite	33.6 V/μm	−118~−1476 mm, 118~1476 mm	185 ms (drive) 296 ms (recover)	Acrylic (VHB 4905)	[84]

5. Applications and Challenges

5.1. Applications

5.1.1. Auto-Zoom Imaging

Auto-zoom systems can sense changes in the environment in real time, intelligently analyse the position and movement of the target object, and adjust the focal length quickly and accurately to ensure that the image remains clear and stable at all times. This system has become a key technology component in many important industries such as consumer electronics, industrial automation, medical equipment, and defence. While traditional autofocus systems mainly rely on complex mechanical structures and motor drives for focus adjustment, the emergence of DETL provides a new solution for the miniaturisation, low power consumption, and high flexibility of autofocus systems. Rasti et al. [85,86] developed a dielectric elastomer-driven passive autofocus system with liquid, as shown in Figure 13a, which identifies the in-focus and out-of-focus images by calculating the standard deviation of the image and then adjusts the voltage to achieve autofocus. The voltage can be adjusted to achieve autofocus. Li et al. [66] developed a dielectric elastomer-driven eye movement lens, which can control the change in the field of view and focal length of the lens by using the electrical signal of eye movement, as shown in Figure 13b, and the zoom ratio can reach 132.6%. Huang et al. [56] developed a dielectric elastomer-driven liquid droplet lens and integrated it into the camera lens of a smartphone. Due to its

lightweight and rapid response advantages, DETL is well-suited to pursuing thin and light smartphone designs. With the continuous improvement of material properties and manufacturing processes, DETL-based auto-zoom imaging systems are expected to achieve a wider zoom range, faster response speed, and better image quality, significantly enhancing the overall performance of smartphone lenses. With its low power consumption and flexible deformation characteristics, this auto-zoom technology is also suitable for portable cameras, endoscopes, smart glasses, and machine vision, among other fields, demonstrating broad application prospects. DETL must accelerate technological breakthroughs in lowering driving voltage, increasing cycle life, and closed-loop control of focal length field to fully capitalise on its advantages.

5.1.2. Microscopic Imaging

Microscopic imaging systems play an irreplaceable role in life sciences, materials research, medical diagnosis, and industrial inspection by their high-precision observation and analysis capabilities. By visualising the details of the microscopic world, microscopic imaging systems not only promote breakthroughs in basic research but also become a core support tool for technological progress and industrial upgrading. Traditional microscopic imaging systems rely on two-stage magnification of the objective lens and eyepiece and usually need to replace the objective lens with a different magnification to achieve zoom. The dielectric elastomer-driven tuneable lens can continuously and smoothly adjust the focal length of the lens by controlling the voltage to constantly zoom in on tiny samples. Hao et al. [58] developed a droplet lens with a zoom ratio of 139.1% and good imaging of biological sample slides. Chen et al. [83] developed a dielectric elastomer-driven Alvarez lens, as shown in Figure 13c, with a zoom magnification of up to 10x and a resolution of up to 114 l p/mm during the zoom process. They also conducted imaging tests on pineal and biointestinal tissue slices at different magnifications, achieving good imaging quality. In the future, the dielectric elastomer-driven microimaging system is expected to be applied in the fields of in vivo cell detection, material structure analysis, and non-destructive testing. To this end, DETL needs to improve its performance in terms of resolution enhancement, aberration correction, and precise control of focal length.

5.1.3. AR Display

The core principle of AR optical devices is to project computer-generated virtual information (e.g., 3D models, text, etc.) into the user's field of view by superimposing it in real time with the real scene using an optical display device through an optical system, forming a visual effect of fusion of reality and virtual reality [87–89]. With virtual-reality symbiosis and real-time interaction, it has great industry, education, and consumption potential. Liu et al. [84] proposed a tuneable planar liquid crystal Alvarez lens based on a DEA, as shown in Figure 13d. They succeeded in dynamically projecting the virtual character's light to depths of 55 cm, 65 cm, and 80 cm in the verification of the AR display. The virtual character 'light' was projected to a depth of 55 cm, 65 cm, and 80 cm in the verification of the AR display, which is a good example of the AR display. 65 cm, 65 cm, and 80 cm in depth, and achieve clear multi-plane fusion with real objects, which provides a new idea for lightweight AR devices. With the advantages of miniaturisation and fast response, dielectric elastomer-driven AR optical devices are expected to be applied in intelligent navigation, virtual meetings, and interactive education scenarios, bringing innovative experiences to various fields. In the future, DETL needs to continue its research in system integration, multisensory coordination, and material performance enhancement.

5.1.4. Infrared Imaging

By detecting infrared radiation emitted by an object and converting it into a temperature distribution image through an infrared detector, the infrared imaging system breaks through the human naked eye's dependence on visible light. It becomes an indispensable sensory tool in modern science and technology [90]. Its unique detection capability in complex environments and non-contact measurement advantages have made it occupy a central position in military, security, industrial, medical, and scientific research. Cheng et al. [91] developed a dielectric elastomer-driven long-wave infrared Alvarez lens based on DE as shown in Figure 13e, with a zoom ratio that continuously covers a dynamically adjustable focal length from $5 \times$ to $15 \times$. Combined with an infrared detector, the system is capable of high-resolution imaging under compact and low-power conditions, providing an innovative solution for miniaturised infrared zoom applications such as unmanned airborne devices and thermal imaging cameras. In the future, the dielectric elastomer-driven infrared imaging system can be applied in UAV reconnaissance, thermal fault warning, driving environment sensing, etc. DETL still needs to improve its performance further in optical performance optimisation and environmental adaptability.

5.2. Challenges

5.2.1. Material Performance Challenges

Although DE has many advantages in tuneable lens applications, current material properties still have limitations in driving performance, stability, durability, and high voltage, which restrict their further development and broad application [92].

Driver performance

At the drive performance level, existing DEA finds reconciling the dual requirements of large deformation and fast response challenging. Studies have shown that DE materials that achieve large optical zoom ratios often require properties of low modulus of elasticity and high dielectric constant. Still, the mechanical response time of such materials is usually large (>100 ms), which cannot meet the response requirements of dynamic target tracking and other scenarios. On the contrary, high-modulus materials reduce the response time, but their magnification ratio is drastically reduced, resulting in a limited optical adjustment range. This inherent contradiction in material performance essentially stems from the dynamics of the polymer chain segments. While low crosslink density materials can achieve large deformations, the viscoelastic dissipation of the molecular chain reconstruction process severely constrains the response speed [93]. Blending materials with low Young's modulus and low dielectric loss [94], along with the addition of plasticisers (such as epoxidised soybean oil) and high dielectric constant fillers, offers potential solutions to the contradiction between fast response and large strain of DE [95].

In addition, the common single-layer planar DEA has significant mechanical performance shortcomings. The equivalent driving force generated by a single-layer DEA film at the driving voltage is a few mN, which may be challenging to overcome the combined resistance generated by the interfacial tension of the liquid lens and the elastic reset mechanism when applied to tuneable lenses with an extensive adjustment range of size or focal length. Therefore, attempts can be made to enhance the driving force by stacking multilayer DEA structures to improve the lens performance [95,96].

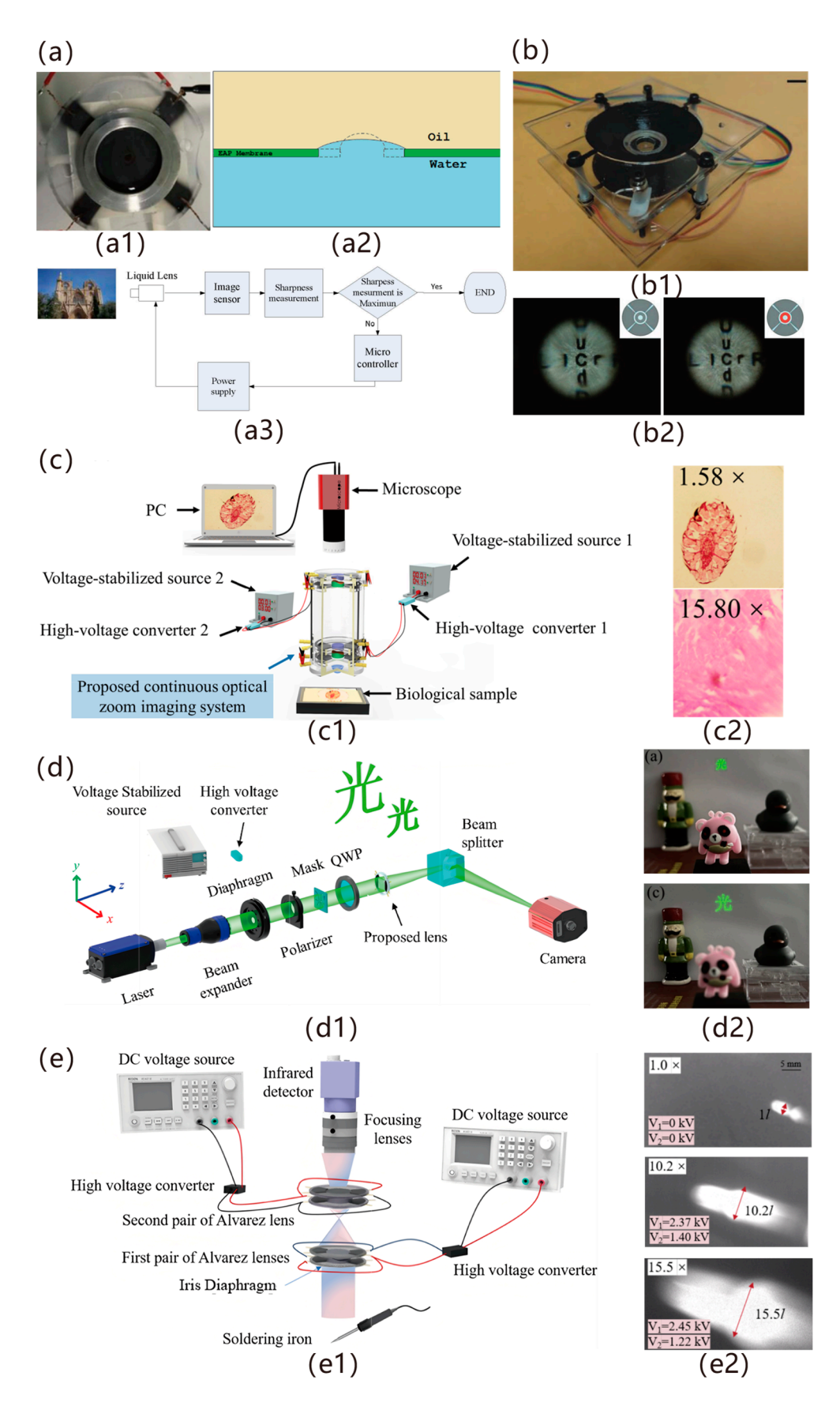


Figure 13. DETL applications. (a) Autofocus systems: (a1) top view of the lens object; (a2) schematic diagram of the lens structure; (a3) schematic diagram of the zoom system [85]. (b) Eye-tracking lenses: (b1) lens physical diagram; (b2) lens zoom effect diagram; the left and right diagrams are the imaging pictures before and after the application of voltage [66]. (c) Microimaging: (c1) system

schematic; (c2) system zoom effect diagram; the upper and lower diagrams are the imaging pictures before and after the voltage change, respectively [83]. (d) AR displays: (d1) system schematic diagram; (d2) AR display effect diagram; the upper and lower diagrams are imaging pictures before and after voltage change, respectively (where '\(\mathcal{L}'\) is the Chinese character for light) [84]. (e) Infrared imaging: (e1) system schematic diagram; (e2) infrared imaging effect picture [91].

2. Material stability

The stability of materials such as DE and drive electrodes is also a key issue. DE materials can also change the electrical and mechanical properties over time due to stress relaxation and other effects after pre-stretching, reducing the stability and reliability of tuneable lenses [97,98]. Carbon grease is widely used as an electrode material for DEAs due to its low price and simple preparation advantages. However, carbon grease electrodes tend to solidify over time, significantly reducing the lens's zoom ratio and affecting the stability of the lens's performance. In addition, hydrogel material has become another research direction of electrode materials due to its high transparency and flexibility. Still, hydrogel has high water absorption, and by absorbing water in the air, the electrical and mechanical properties of the electrode are changed, which further affects the performance stability of the tuneable lens. Meanwhile, the stability of the internal liquid or soft solid material when DEs are used as actuators must also be considered [99].

3. Material durability

The durability of the lens mainly depends on the performance retention of the DE, and the decline of its mechanical properties during repeated driving is a problem that should not be ignored. In practical applications, tuneable lenses frequently change the focal length, requiring DE to withstand repeated mechanical effects such as stretching and compression. However, the mechanical properties of DE are relatively weak and prone to fatigue problems under repeated driving over a long period [100].

Fatigue is a phenomenon in which a DE is subjected to the mechanical action of cyclic loading. Microcracks gradually develop and expand within the material, ultimately degrading the material's properties. When a DEA drives a tuneable lens, each time a voltage is applied and removed, the dielectric elastomer undergoes a cycle of stretching and recovery. As cycles increase, microcracks within the DE accumulate, which reduces the material's strength and toughness. Studies have shown that the tensile strength of some DE may decrease after tens of thousands of cycle drives [92,101]. This fatigue phenomenon affects the driving performance of DE. It may cause the lens to fail to accurately reach the preset focal length during the zoom process, making the picture blurred and distorted. This is an urgent problem for tuneable lens applications that require long-term stable operation. To improve the service life of DETL, it is necessary to develop DE materials with higher durability or to reduce the stresses that DE are subjected to during the driving process by improving the structural design and optimising the driving method to reduce the occurrence of the mechanical property degradation [102,103].

4. High drive voltage

Currently, commonly used DE materials, such as PDMS, generally have a low relative dielectric constant of around 2–3. This makes it often necessary to apply driving voltages in the thousands of volts to achieve the deformation required by DE to drive tuneable lenses in practical applications. Such high drive voltages pose several problems. Firstly, the generation and control of high voltages requires complex and expensive power supply equipment, which increases the cost and size of the system, limiting the use of tuneable lenses in several size- and cost-sensitive application scenarios, such as portable imaging devices,

endoscopic probes, and so on. Secondly, high voltage also poses a safety hazard. When the applied voltage exceeds the breakdown field strength of the DE, a conductive channel will be formed inside the DE, leading to material damage and preventing the tuneable lens from functioning correctly, which reduces the reliability and stability of the system. At the same time, the high voltage also challenges the research of its DETL self-sensing technology. The self-sensing technology mainly predicts strain by measuring the current capacitance value of DEA, but during the measurement of DEA capacitance, the high-voltage environment makes it difficult for most capacitance sensors to be appropriately applied, and special circuits need to be prepared, which restricts the effective implementation of the relevant technical solutions [104,105].

5.2.2. Modelling and Control Challenges

Dielectric elastomer modelling complexity

Dielectric elastomers exhibit complex dynamic nonlinear behaviours, such as hysteresis, rate correlation, temperature, and load effects, leading to multifaceted challenges in the focus control of tuneable lenses driven by them. Regarding static performance, the lens's focal length change is more linear at low voltage, whereas it is significantly nonlinear and accelerated at high voltage. Regarding dynamic response, the hysteresis effect causes a delay in focal length adjustment, which impacts control accuracy and response speed [106,107]. This nonlinear behaviour reduces the imaging quality of high-precision imaging systems and also results in blurring during high-speed imaging. Meanwhile, the nonlinear modelling of dielectric elastomers is influenced by multiple factors such as stress, temperature, and electric field. It is closely related to its initial state, deformation history, and material type. Although considerable research and progress have been made in modelling to predict the nonlinear properties of dielectric elastomers, the models still face numerous challenges in terms of accuracy, long-term performance, and generalisability [108].

Control system challenges

Current DETLs are primarily controlled using open-loop systems, largely due to the difficulties of obtaining accurate feedback signals for focal length. Developing an effective feedback control scheme presents a core challenge for achieving precise focus adjustment of DETL. In the case of liquid lenses, changes in hydraulic pressure can be employed as the feedback signal. In contrast, displacement zoom-based DETL determines the lens position in real time through sensors and achieves closed-loop focus control by integrating with a dynamic model [109].

The accuracy of the DETL control system is significantly affected by variations in material parameters over time. In the pre-stretched state, the dielectric elastomer's elastic modulus and dielectric constant gradually change due to stress relaxation, leading to the failure of the original control parameters. This, in turn, affects the driving effect and focus control accuracy. If the system cannot be adjusted promptly, it may result in issues such as reducing focal length adjustment accuracy. Furthermore, in the face of vibrations and other complex environments [110], designing the control system to enhance the imaging stability of the lens, combined with the lens model, and utilising the control algorithm to improve the lens's response time remains a current challenge [111,112].

5.2.3. Preparation Process Challenges

The fabrication process of DETL is complex and consists of three key aspects: prestretching, precise electrode preparation, and lens moulding. Pre-stretching requires control of mechanical uniformity and interfacial bonding; electrode preparation necessitates accurate control of thickness and pattern [113]; and lens moulding presents challenges such as mould surface treatment and liquid injection sealing [114]. Current processes rely on Appl. Sci. 2025, 15, 6926 23 of 29

manual operation, resulting in long preparation cycles and poor batch-to-batch repeatability, which limits large-scale efficiency production [115,116].

In addition, when integrating a tuneable lens into a camera lens, it is necessary to ensure that the lens and other optical components of the camera can be accurately aligned and maintain a stable relative position during operation. Since DE can deform under the action of an electric field, this may change the relative position between the lens and the other components, thereby affecting the quality of the image.

5.2.4. Optical Performance Challenges

Tuneable lenses may introduce a variety of optical aberrations, such as spherical aberration, coma, etc., during the deformation process, which can significantly affect the performance of the imaging system and lead to a decrease in the clarity and accuracy of the images. The existence of such aberrations greatly limits the application of DETL in fields with high imaging quality requirements, such as high-precision microscopic imaging and astronomical observation. In the current design structure of most tuneable lenses, a single electrode region is usually used for open-loop control, which cannot adjust the morphology of the lens in real time or dynamically according to the detected aberration, and it is difficult to achieve adequate compensation and optimisation of the aberration. As a result, the non-ideal morphology produced by the lens during the deformation process cannot be corrected in time, which directly affects the imaging quality [18]. The active aberration adjustment can be accomplished by designing a multi-electrode region [49]. Real-time compensation for aberration based on this scheme can further enhance the imaging quality of the lens.

Additionally, existing tuneable lenses based on dielectric elastomer actuation still face limitations regarding zoom range. Currently, the zoom ratio of dielectric elastomer-driven liquid lenses is typically only a few times, which makes it challenging to meet the demand for high-magnification zoom in certain specialised fields such as telephoto photography, astronomical observation, and telephoto imaging. Consequently, there is an urgent need to explore new driving principles and design methods to achieve adjustable focus technologies with higher resolution and greater adjustment capability range.

6. Conclusions

DETL has made notable progress as an innovative optical component in recent years. In this review, DETLs based on various driving principles and structural designs are systematically organised, and their technical characteristics, application potentials, and development challenges are analysed in depth to provide theoretical support and practical references for the optimal design of optical systems.

According to the tuning mechanism, DETL can be classified into two types: zoom by anamorphic zoom and zoom by displacement zoom. Deformation zoom is achieved by directly or indirectly changing the shape of the lens through DEA, and displacement zoom is mainly achieved by changing the object distance and image distance through DEA. In terms of composition, monolithic, composite, array, and metal lenses have their own characteristics.

Meanwhile, the performances of some publicly reported liquid prisms are analysed and compared, with the expectation of providing readers with a reference for choosing liquid prisms. Also, an overview of the applications of DETL, a lens that can be used in auto-zoom imaging systems, microscopic imaging, AR displays, and infrared imaging, is presented.

However, the technology still faces many challenges. Regarding material properties, the contradiction between large strain and fast response, as well as the lack of stability and

Appl. Sci. 2025, 15, 6926 24 of 29

durability, limits further improvement of lens performance. In terms of modelling and control, the strong nonlinear characteristics of dielectric elastomers hinder precise control of the focal length, and the constant changes in model parameters lead to a lack of long-term stability in the controller. Concerning the preparation process, the complexity of the steps and manual preparation affect the efficiency of experiments and parallelism. Additionally, regarding optical performance, the uneven deformation of dielectric elastomers causes issues like spherical aberration, which impacts imaging quality. Moreover, the existing zoom capability of DETL still falls short of meeting the demand for greater magnification zoom.

Author Contributions: Conceptualisation, Z.H. and H.H.; methodology, Z.H. and H.H.; investigation, Z.H., M.Z., Z.G., and J.L.; writing—original draft preparation, Z.H., J.L., and Z.L.; writing—review and editing, M.Z. and Z.G.; visualisation, Z.H. and Z.L.; supervision, H.H.; project administration, M.Z. and Z.G.; funding acquisition, H.H. and M.Z. All authors have read and agreed to the published version of the manuscript.

Funding: This research received no external funding.

Institutional Review Board Statement: Not applicable.

Informed Consent Statement: Not applicable.

Data Availability Statement: The raw data supporting the conclusions of this article will be made available by the authors on request.

Conflicts of Interest: The authors declare no conflicts of interest.

References

- Yang, Z.; Liu, L.; Li, Z.; Jiao, Y.; Zhang, L.; Cui, Y. A Magnetically-Actuated Ultrasound Capsule Endoscope (MUSCE) for Endoluminal Imaging in Tubular Environments. *IEEE Robot. Autom. Lett.* 2025, 10, 2590–2597. [CrossRef]
- 2. Ge, J.; Qin, Y.; Liu, X.; Tang, X. Design of Variable Spot and Zoom Optical System for Laser Cutting. *Acta Opt. Sin.* **2019**, 39, 222001. [CrossRef]
- 3. Fu, Q.; Ma, N.; Liu, X.; Zhang, Y.; Zhan, J.; Zhang, S.; Duan, J.; Li, Y. Analysis of Multispectral Polarization Imaging Image Information Based on Micro-Polarizer Array. *PLoS ONE* **2024**, *19*, e0296397. [CrossRef] [PubMed]
- 4. Lin, Y.-H.; Chen, M.-S.; Lin, H.-C. An Electrically Tunable Optical Zoom System Using Two Composite Liquid Crystal Lenses with a Large Zoom Ratio. *Opt. Express* **2011**, *19*, 4714. [CrossRef] [PubMed]
- Liu, C.; Shi, G. General Situations of Mechanical Compensation Zoom Lens in Its Three Development Phases and Its Developing Direction. J. Appl. Opt. 1992, 1, 15–19.
- 6. Smith, W.J. Optical Engineering: The Design of Optical Systems, 4th ed.; McGraw-Hill: New York, NY, USA, 2008; ISBN 978-0-07-147687-4.
- 7. Liu, C.; Zheng, Y.; Yuan, R.; Jiang, Z.; Xu, J.; Zhao, Y.; Wang, X.; Li, X.; Xing, Y.; Wang, Q. Tunable Liquid Lenses: Emerging Technologies and Future Perspectives. *Laser Photonics Rev.* **2023**, *17*, 2300274. [CrossRef]
- 8. Xu, S.; Li, Y.; Liu, Y.; Sun, J.; Ren, H.; Wu, S.-T. Fast-Response Liquid Crystal Microlens. *Micromachines* **2014**, *5*, 300–324. [CrossRef]
- 9. Lin, Y.-H.; Wang, Y.-J.; Reshetnyak, V. Liquid Crystal Lenses with Tunable Focal Length. *Liq. Cryst. Rev.* **2017**, *5*, 111–143. [CrossRef]
- 10. Zheng, Y.; Zhang, H.-R.; Li, X.-W.; Zhao, Y.-R.; Li, Z.-S.; Hou, Y.-H.; Liu, C.; Wang, Q.-H. Fast-Zoom and High-Resolution Sparse Compound-Eye Camera Based on Dual-End Collaborative Optimization. *Opto-Electron. Adv.* **2025**, *8*, 240285. [CrossRef]
- 11. Hasan, N.; Kim, H.; Mastrangelo, C.H. Large Aperture Tunable-Focus Liquid Lens Using Shape Memory Alloy Spring. *Opt. Express* **2016**, 24, 13334. [CrossRef]
- 12. Youn, J.-H.; Hyeon, K.; Ma, J.H.; Kyung, K.-U. A Piecewise Controllable Tunable Lens with Large Aperture for Eyewear Application. *Smart Mater. Struct.* **2019**, *28*, 124001. [CrossRef]
- 13. Wapler, M.C.; Sturmer, M.; Wallrabe, U. A Compact, Large-Aperture Tunable Lens with Adaptive Spherical Correction. In Proceedings of the 2014 International Symposium on Optomechatronic Technologies, Seattle, WA, USA, 5–7 November 2014; IEEE: New York, NY, USA, 2014; pp. 130–133.

Appl. Sci. **2025**, 15, 6926 25 of 29

14. Wang, L.; Ishikawa, M. Dynamic Response of Elastomer-Based Liquid-Filled Variable Focus Lens. *Sensors* **2019**, *19*, 4624. [CrossRef] [PubMed]

- 15. Nicolas, S.; Allain, M.; Bridoux, C.; Fanget, S.; Lesecq, S.; Zarudniev, M.; Bolis, S.; Pouydebasque, A.; Jacquet, F. Fabrication and Characterization of a New Varifocal Liquid Lens with Embedded PZT Actuators for High Optical Performances. In Proceedings of the 2015 28th IEEE International Conference on Micro Electro Mechanical Systems (MEMS), Estoril, Portugal, 18–22 January 2015; IEEE: New York, NY, USA, 2015; pp. 65–68.
- 16. Wakle, S.; Lin, T.-H.; Huang, S.; Basu, S.; Lau, G.-K. How Fast Can a Robotic Drummer Beat Using Dielectric Elastomer Actuators? *IEEE Robot. Autom. Lett.* **2024**, *9*, 2638–2645. [CrossRef]
- 17. Huang, J.; Zhang, X.; Liu, R.; Ding, Y.; Guo, D. Polyvinyl Chloride-Based Dielectric Elastomer with High Permittivity and Low Viscoelasticity for Actuation and Sensing. *Nat. Commun.* **2023**, *14*, 1483. [CrossRef] [PubMed]
- 18. Chen, L.; Ghilardi, M.; Busfield, J.J.C.; Carpi, F. Electrically Tunable Lenses: A Review. Front. Robot. Al 2021, 8, 678046. [CrossRef]
- 19. Yang, L.; Wang, H.; Zhang, D.; Yang, Y.; Leng, D. Large Deformation, High Energy Density Dielectric Elastomer Actuators: Principles, Factors, Optimization, Applications, and Prospects. *Chem. Eng. J.* **2024**, 489, 151402. [CrossRef]
- 20. Pelrine, R.E.; Kornbluh, R.D.; Joseph, J.P. Electrostriction of Polymer Dielectrics with Compliant Electrodes as a Means of Actuation. *Sens. Actuators A Phys.* **1998**, *64*, 77–85. [CrossRef]
- 21. Pelrine, R.; Kornbluh, R.D.; Eckerle, J.; Jeuck, P.; Oh, S.; Pei, Q.; Stanford, S. Dielectric Elastomers: Generator Mode Fundamentals and Applications. In *Smart Structures and Materials 2001: Electroactive Polymer Actuators and Devices, Proceedings of the SPIE's 8th Annual International Symposium on Smart Structures and Materials, Newport Beach, CA, USA, 4–8 March 2001*; Bar-Cohen, Y., Ed.; SPIE: San Diego, CA, USA, 2001; p. 148.
- 22. Lu, T.; Ma, C.; Wang, T. Mechanics of Dielectric Elastomer Structures: A Review. Extrem. Mech. Lett. 2020, 38, 100752. [CrossRef]
- 23. Liang, X.; Cai, S. New Electromechanical Instability Modes in Dielectric Elastomer Balloons. *Int. J. Solids Struct.* **2018**, 132–133, 96–104. [CrossRef]
- 24. Yang, L.; Hao, M.; Yang, K.; Lan, D.; Zhang, X.; Tian, X.; Wang, Z. A Review of Methods and Applications for Improving Electric Driving Performance of Dielectric Elastomer. *IEEE Trans. Dielectr. Electr. Insul.* **2025**, *32*, 117–126. [CrossRef]
- Tang, C.; Du, B.; Jiang, S.; Wang, Z.; Liu, X.-J.; Zhao, H. A Review on High-frequency Dielectric Elastomer Actuators: Materials, Dynamics, and Applications. Adv. Intell. Syst. 2024, 6, 2300047. [CrossRef]
- 26. Huang, W.; Chen, K.; Ma, P.; Kang, G. A Visco-Hyperelastic Constitutive Model for Temperature-Dependent Cyclic Deformation of Dielectric Elastomer. *Acta Mech. Solida Sin.* **2024**, *37*, 736–749. [CrossRef]
- 27. Gao, L.; Zhang, Y.; Xiao, Q.; Gao, Z.; Wang, X. Optimizing Energy Storage Density of the Multi–Layer Composite of Poly(Vinylidene Fluoride) and Nano–Ni Plated CaCu₃Ti₄O₁₂ with an Ultralow Filling Content. *Compos. Sci. Technol.* **2024**, 245, 110353. [CrossRef]
- 28. Liu, L.; Zhang, K.; Liu, J.; Zhu, L.; Xie, R.; Lv, S. Significant Improvements in the Electromechanical Performance of Dielectric Elastomers by Introducing Ternary Dipolar Groups. *React. Funct. Polym.* **2022**, *172*, 105177. [CrossRef]
- 29. Hecht, E. Optics, 4th ed.; Addison-Wesley: Boston, MA, USA, 2002; ISBN 978-0-8053-8566-3.
- 30. Carpi, F.; Frediani, G.; Turco, S.; De Rossi, D. Bioinspired Tunable Lens with Muscle-like Electroactive Elastomers. *Adv. Funct. Mater.* **2011**, *21*, 4152–4158. [CrossRef]
- 31. Pieroni, M.; Lagomarsini, C.; De Rossi, D.; Carpi, F. Electrically Tunable Soft Solid Lens Inspired by Reptile and Bird Accommodation. *Bioinspiration Biomim.* **2016**, *11*, 65003. [CrossRef]
- 32. Son, S.; Pugal, D.; Hwang, T.; Choi, H.R.; Koo, J.C.; Lee, Y.; Kim, K.; Nam, J.-D. Electromechanically Driven Variable-Focus Lens Based on Transparent Dielectric Elastomer. *Appl. Opt.* **2012**, *51*, 2987. [CrossRef]
- 33. Keong, G.-K.; La, T.-G.; Shiau, L.-L.; Tan, A.W.Y. Challenges of Using Dielectric Elastomer Actuators to Tune Liquid Lens. In Electroactive Polymer Actuators and Devices (EAPAD) 2014, Proceedings of the SPIE Smart Structures and Materials + Nondestructive Evaluation and Health Monitoring, San Diego, CA, USA, 9–13 March 2014; Bar-Cohen, Y., Ed.; SPIE: San Diego, CA, USA, 2014; p. 90561J.
- 34. Zhang, H.; Zhang, Z. Modeling of Lens Based on Dielectric Elastomers Coupling with Hydrogel Electrodes. In *Mechatronics and Machine Vision in Practice 4*; Springer International Publishing: Cham, Switzerland, 2021; pp. 263–268. ISBN 978-3-030-43702-2.
- 35. Wei, K.; Domicone, N.W.; Zhao, Y. Electroactive Liquid Lens Driven by an Annular Membrane. *Opt. Lett.* **2014**, *39*, 1318. [CrossRef]
- 36. Cheng, Y.; Cao, J.; Wang, Y.; Ning, Y.; Hao, Q. Design and Analysis of Liquid Lens Driven by Dielectric Elastomer. *Acta Opt. Sin.* **2021**, 41, 164–173. [CrossRef]
- 37. Shi, H.; Wang, H. Modelling of a Soft Tunable Lens Actuated by an Annular Dielectric Elastomer Actuator with Homogeneous and Inhomogeneous Prestretches. *J. Phys. D Appl. Phys.* **2021**, *54*, 245402. [CrossRef]

Appl. Sci. 2025, 15, 6926 26 of 29

38. Kim, H.; Park, J.; Chuc, N.H.; Choi, H.R.; Nam, J.D.; Lee, Y.; Jung, H.S.; Koo, J.C. Development of Dielectric Elastomer Driven Micro-Optical Zoom Lens System. In *Electroactive Polymer Actuators and Devices (EAPAD)* 2007, *Proceedings of the SPIE Smart Structures and Materials* + *Nondestructive Evaluation and Health Monitoring, San Diego, CA, USA,* 18–22 March 2007; Bar-Cohen, Y., Ed.; SPIE: San Diego, CA, USA, 2007; p. 65241V.

- 39. Yun, S.; Park, S.; Park, B.; Nam, S.; Park, S.K.; Kyung, K.-U. A Thin Film Active-Lens with Translational Control for Dynamically Programmable Optical Zoom. *Appl. Phys. Lett.* **2015**, *107*, 81907. [CrossRef]
- 40. Jin, B.; Ren, H. Position-Movable Lens Driven by Dielectric Elastomer Actuator. Opt. Eng. 2016, 55, 075101. [CrossRef]
- 41. Rastani, K.; Marrakchi, A.; Habiby, S.F.; Hubbard, W.M.; Gilchrist, H.; Nahory, R.E. Binary Phase Fresnel Lenses for Generation of Two-Dimensional Beam Arrays. *Appl. Opt.* **1991**, *30*, 1347. [CrossRef]
- 42. Park, S.; Park, B.; Nam, S.; Yun, S.; Park, S.K.; Mun, S.; Lim, J.M.; Ryu, Y.; Song, S.H.; Kyung, K.-U. Electrically Tunable Binary Phase Fresnel Lens Based on a Dielectric Elastomer Actuator. *Opt. Express* **2017**, *25*, 23801. [CrossRef] [PubMed]
- 43. Alvarez, L. Two-Element Variable-Power Spherical Lens. U.S. Patent No. 3,305,294, 21 February 1967.
- 44. Cheng, Y.; Chen, C.; Li, Z.; Yan, Z.; Cao, J.; Hao, Q. Experimental Study on the Focal Length of Alvarez Lens Actuated by Dielectric Elastomer with Different Pre-Stretched Ratios and Diameters. In *Optical Design and Testing XII*, *Proceedings of the SPIE/Cos Photonics Asia*, *Beijing*, *China*, 5–12 *December* 2022; Wu, R., Wang, Y., Kidger, T.E., Eds.; SPIE: San Diego, CA, USA, 2022; p. 22.
- 45. Hao, Q.; Chen, C.; Cao, J.; Li, Z.; Cheng, Y. Ultra-Wide Varifocal Imaging with Selectable Region of Interest Capacity Using Alvarez Lenses Actuated by a Dielectric Elastomer. *Photon. Res.* **2022**, *10*, 1543. [CrossRef]
- 46. Kim, B.-C.; Lee, Y.; Nam, J.-D.; Moon, H.; Choi, H.R.; Koo, J.C. Smart Material Actuators for Micro Optical Zoom Lens Driving Systems. *IEEE Trans. Magn.* **2011**, 47, 1999–2004. [CrossRef]
- 47. Nam, S.; Yun, S.; Yoon, J.W.; Park, S.; Park, S.K.; Mun, S.; Park, B.; Kyung, K.-U. A Robust Soft Lens for Tunable Camera Application Using Dielectric Elastomer Actuators. *Soft Rob.* **2018**, *5*, 777–782. [CrossRef] [PubMed]
- 48. Chen, B.; Sun, W.; Lu, J.; Yang, J.; Chen, Y.; Zhou, J.; Suo, Z. All-Solid Ionic Eye. J. Appl. Mech. 2021, 88, 31016. [CrossRef]
- 49. Ghilardi, M.; Boys, H.; Török, P.; Busfield, J.J.C.; Carpi, F. Smart Lenses with Electrically Tuneable Astigmatism. *Sci. Rep.* **2019**, 9, 16127. [CrossRef]
- 50. Maffli, L.; Rosset, S.; Ghilardi, M.; Carpi, F.; Shea, H. Ultrafast All-polymer Electrically Tunable Silicone Lenses. *Adv. Funct. Mater.* **2015**, 25, 1656–1665. [CrossRef]
- 51. Wang, Y.; Li, P.; Gupta, U.; Ouyang, J.; Zhu, J. Tunable Soft Lens of Large Focal Length Change. *Soft Robot.* **2022**, *9*, 705–712. [CrossRef] [PubMed]
- 52. Lu, T.; Cai, S.; Wang, H.; Suo, Z. Computational Model of Deformable Lenses Actuated by Dielectric Elastomers. *J. Appl. Phys.* **2013**, *114*, 104104. [CrossRef]
- 53. Wang, Q.; Cao, Y.J.; Wang, Y.N.; Liu, J.C.; Xie, Y.-X. A Computational Model of Bio-Inspired Tunable Lenses. *Mech. Based Des. Struct. Mach.* 2018, 46, 800–808. [CrossRef]
- 54. Liu, S.; Qiu, Y.; Yu, W. Self-contained Focus-tunable Lenses Based on Transparent and Conductive Gels. *Macromol. Mater. Eng.* **2020**, *305*, 2000393. [CrossRef]
- 55. Jin, B.; Lee, J.-H.; Zhou, Z.; Zhang, G.; Lee, G.-B.; Ren, H.; Nah, C. Adaptive Liquid Lens Driven by Elastomer Actuator. *Opt. Eng.* **2016**, *55*, 17107. [CrossRef]
- 56. Huang, H.; Zhao, Y. Smartphone Based Focus-free Macroscopy Using An Adaptive Droplet Lens. In Proceedings of the 2018 Solid-State, Actuators, and Microsystems Workshop Technical Digest, Hilton Head, SC, USA, 3–7 June 2018; Transducer Research Foundation: San Diego, CA, USA, 2018; pp. 334–337.
- 57. Cheng, Y.; Li, Z.; Chen, C.; Ning, Y.; Cao, J.; Liu, L.; Hao, Q. Varifocal Liquid Lens Driven by Dielectric Elastomer with Different Pre-Stretched Ratios. In *Optical Design and Testing XII, Proceedings of the SPIE/Cos Photonics Asia, Beijing, China, 5–12 December* 2022; Wu, R., Wang, Y., Kidger, T.E., Eds.; SPIE: San Diego, CA, USA, 2022; p. 48.
- 58. Hao, Q.; Li, Z.; Chen, C.; Cao, J.; Cheng, Y. Adaptive Liquid Lens Actuated by Dielectric Elastomer with Transparent Conductive Droplet. In *Optical Design and Testing XI, Proceedings of the SPIE/Cos Photonics Asia, Nantong, China, 10–20 October 2021*; Wu, R., Matoba, O., Wang, Y., Kidger, T.E., Eds.; SPIE: San Diego, CA, USA, 2021; p. 33.
- 59. Liang, D.; Lin, Z.; Huang, C.; Shih, W. Tunable Lens Driven by Dielectric Elastomer Actuator with Ionic Electrodes. *Micro Nano Lett.* **2014**, *9*, 869–873. [CrossRef]
- 60. Shian, S.; Diebold, R.M.; Clarke, D.R. High-speed, compact, adaptive lenses using in-line transparent dielectric elastomer actuator membranes. In *Electroactive Polymer Actuators and Devices (EAPAD)* 2013, *Proceedings of the SPIE Smart Structures And Materials* + *Nondestructive Evaluation And Health Monitoring, San Diego, CA, USA,* 10–14 March 2013; Bar-Cohen, Y., Ed.; SPIE: San Diego, CA, USA, 2013; p. 86872D.
- 61. Cheng, Y.; Chen, C.; Cao, J.; Bao, C.; Yang, A.; Hao, Q. Tunable Lens Using Dielectric Elastomer Sandwiched by Transparent Conductive Liquid. *Opt. Lett.* **2021**, *46*, 4430. [CrossRef]

Appl. Sci. **2025**, 15, 6926 27 of 29

62. Hao, Q.; Chen, C.; Li, Z.; Cao, J.; Cheng, Y. Optofluidic Varifocal Lens Actuated by Dielectric Elastomer Sandwiched by Two Conductive Liquids with Different Refractive Indexes. In *Advanced Optical Imaging Technologies IV, Proceedings of the SPIE/Cos Photonics Asia, Nantong, China, 10–20 October 2021*; SPIE: San Diego, CA, USA, 2021; Volume 11896, pp. 8–15.

- 63. Zhang, C.; He, H.; Li, Y.; Sun, Y.; Dong, Z. Modeling and Design of Dielectric Elastomer Actuated Tunable Lens with Dual Chambers. *AIP Adv.* 2022, 12, 075119. [CrossRef]
- 64. Shian, S.; Diebold, R.M.; Clarke, D.R. Tunable Lenses Using Transparent Dielectric Elastomer Actuators. *Opt. Express* **2013**, 21, 8669. [CrossRef]
- 65. Cao, Y.; Wang, Y.; Liu, Y.; Xie, Y.-X. Explicit Computational Model of Dielectric Elastomeric Lenses: Erratum. *Opt. Express* **2019**, 27, 37834. [CrossRef]
- 66. Li, J.; Wang, Y.; Liu, L.; Xu, S.; Liu, Y.; Leng, J.; Cai, S. A Biomimetic Soft Lens Controlled by Electrooculographic Signal. *Adv. Funct. Mater.* **2019**, 29, 1903762. [CrossRef]
- 67. Li, J.; Lv, X.; Liu, L.; Liu, Y.; Leng, J. Computational Model and Design of the Soft Tunable Lens Actuated by Dielectric Elastomer. *J. Appl. Mech.* **2020**, *87*, 071005. [CrossRef]
- 68. Hu, Z.; Zhang, M.; Gan, Z.; Lv, J.; Liu, Z.; Yang, M.; Hong, H. Design and Performance Study of Dielectric Elastomer-Driven Conical Tunable Soft Lens. In *Tenth Symposium on Novel Optoelectronic Detection Technology and Applications, Proceedings of the Tenth Symposium On Novel Optoelectronic Detection Technology And Applications (NDTA 2024), Taiyuan, China, 1–3 November 2024;* Ping, C., Ed.; SPIE: San Diego, CA, USA, 2024; pp. 478–485.
- 69. Yin, X.; Zhou, P.; Wen, S.; Zhang, J. Origami Improved Dielectric Elastomer Actuation for Tunable Lens. *IEEE Trans. Instrum. Meas.* **2022**, 71, 1–9. [CrossRef]
- 70. Yun, S.; Park, S.; Nam, S.; Park, B.; Park, S.K.; Mun, S.; Lim, J.M.; Kyung, K.-U. An Electro-Active Polymer Based Lens Module for Dynamically Varying Focal System. *Appl. Phys. Lett.* **2016**, *109*, 141908. [CrossRef]
- 71. Pu, J.; Meng, Y.; Xie, Z.; Peng, Z.; Wu, J.; Shi, Y.; Plamthottam, R.; Yang, W.; Pei, Q. A Unimorph Nanocomposite Dielectric Elastomer for Large Out-of-Plane Actuation. *Sci. Adv.* **2022**, *8*, eabm6200. [CrossRef]
- 72. Niklaus, M.; Shea, H. Electrically Tunable PDMS Lenses Using Integrated Mm-Scale Dielectric Elastomer Actuators. In Proceedings of the 12th International Conference on New Actuators, Bremen, Germany, 14–16 June 2010.
- 73. Wang, L.; Hayakawa, T.; Ishikawa, M. Dielectric-Elastomer-Based Fabrication Method for Varifocal Microlens Array. *Opt. Express* **2017**, 25, 31708. [CrossRef]
- 74. Chen, C.; Hao, Q.; Liu, L.; Cao, J.; Qiao, Z.; Cheng, Y. Continuous Optical Zoom Compound Eye Imaging Using Alvarez Lenses Actuated by Dielectric Elastomers. *Biomimetics* **2024**, *9*, 374. [CrossRef]
- 75. Wang, H.-W.; Chang, I.-L.; Chen, L.-W. Beam Manipulating by Graded Photonic Crystal Slab Made of Dielectric Elastomer Actuators. *Opt. Commun.* **2012**, *285*, 5524–5530. [CrossRef]
- 76. Pan, M.; Fu, Y.; Zheng, M.; Chen, H.; Zang, Y.; Duan, H.; Li, Q.; Qiu, M.; Hu, Y. Dielectric Metalens for Miniaturized Imaging Systems: Progress and Challenges. *Light Sci. Appl.* **2022**, *11*, 195. [CrossRef]
- 77. She, A.; Zhang, S.; Shian, S.; Clarke, D.R.; Capasso, F. Adaptive Metalenses with Simultaneous Electrical Control of Focal Length, Astigmatism, and Shift. *Sci. Adv.* **2018**, *4*, eaap9957. [CrossRef]
- 78. Hwang, T.; Kwon, H.-Y.; Oh, J.-S.; Hong, J.-P.; Hong, S.-C.; Lee, Y.; Ryeol Choi, H.; Jin Kim, K.; Hossain Bhuiya, M.; Nam, J.-D. Transparent Actuator Made with Few Layer Graphene Electrode and Dielectric Elastomer, for Variable Focus Lens. *Appl. Phys. Lett.* **2013**, *103*, 023106. [CrossRef]
- 79. Jin, B.; Lee, J.-H.; Zhou, Z.; Lee, G.-B.; Ren, H.; Nah, C. Liquid Lens Driven by Elastomer Actuator. In *Zoom Lenses, Proceedings of the SPIE Optical Engineering + Applications, San Diego, CA, USA, 9–13 August 2015*; Betensky, E., Yamanashi, T., Eds.; SPIE: San Diego, CA, USA, 2015; p. 95800O.
- 80. Park, B.J.; Park, S.; Choi, M.; Park, S.K.; Yun, S.; Shin, E.; Yoon, J.W. Monolithic Focus-Tunable Lens Technology Enabled by Disk-Type Dielectric-Elastomer Actuators. *Sci. Rep.* **2020**, *10*, 16937. [CrossRef] [PubMed]
- 81. Jiang, L.; Wang, Y.; Wang, X.; Ning, F.; Wen, S.; Zhou, Y.; Chen, S.; Betts, A.; Jerrams, S.; Zhou, F.-L. Electrohydrodynamic Printing of a Dielectric Elastomer Actuator and Its Application in Tunable Lenses. *Compos. Part A Appl. Sci. Manuf.* **2021**, 147, 106461. [CrossRef]
- 82. Chen, C.; Hao, Q.; Cao, J.; Xu, Y.; Cheng, Y. Two-Dimensional Varifocal Scanning Imaging Based on Alvarez and Decentred Lenses Actuated by Dielectric Elastomer. *Opt. Laser Technol.* **2023**, *167*, 109805. [CrossRef]
- 83. Chen, C.; Hao, Q.; Liu, L.; Cao, J.; Zhang, Y.; Cheng, Y. 10× Continuous Optical Zoom Imaging Using Alvarez Lenses Actuated by Dielectric Elastomers. *Opt. Express* **2024**, *32*, 1246. [CrossRef]
- 84. Liu, L.; Hao, Q.; Li, Z.; Xiong, J.; Zhang, Y.; Cheng, Y. Design and Demonstration of DEA-Based Tunable Planar Liquid Crystal Alvarez Lenses. *Opt. Laser Technol.* **2025**, *182*, 112068. [CrossRef]
- 85. Rasti, P.; Kiefer, R.; Anbarjafari, G. Autofocus Liquid Lens by Using Sharpness Measurement. In Proceedings of the 2015 23nd Signal Processing and Communications Applications Conference (SIU), Malatya, Turkey, 16–19 May 2015; IEEE: New York, NY, USA, 2015; pp. 608–611.

Appl. Sci. 2025, 15, 6926 28 of 29

86. Rasti, P.; Kesküla, A.; Haus, H.; Schlaak, H.F.; Anbarjafari, G.; Aabloo, A.; Kiefer, R. A Passive Autofocus System by Using Standard Deviation of the Image on a Liquid Lens. In *Electroactive Polymer Actuators and Devices (EAPAD)* 2015, *Proceedings of the SPIE Smart Structures and Materials* + *Nondestructive Evaluation and Health Monitoring, San Diego, CA, USA,* 8–12 *March* 2015; Bar-Cohen, Y., Ed.; SPIE: San Diego, CA, USA, 2015; p. 94301Q.

- 87. Chang, Y.K.; Lim, J.; Burkland, J. How Can AR-Enhanced Books Support Early Readers? Exploring Literacy Development through AR Design Principles. *Int. J. Child-Comput. Interact.* **2024**, 42, 100701. [CrossRef]
- 88. Na, H.C.; Kim, Y.S. Study on an Ar-Based Circuit Practice. Appl. Comput. Sci. 2024, 20, 17–27. [CrossRef]
- 89. Lv, C.; Liu, B.; Wu, D.; Lv, J.; Li, J.; Bao, J. AR-Assisted Assembly Method Based on Instance Segmentation. *Int. J. Comput. Integr. Manuf.* **2025**, *38*, 271–287. [CrossRef]
- 90. Kulkarni, N.N.; Raisi, K.; Valente, N.A.; Benoit, J.; Yu, T.; Sabato, A. Deep Learning Augmented Infrared Thermography for Unmanned Aerial Vehicles Structural Health Monitoring of Roadways. *Autom. Constr.* **2023**, *148*, 104784. [CrossRef]
- 91. Cheng, Y.; OuYang, Q.; Yao, C.; Liu, L.; Li, Z.; Hao, Q. Dielectric-Elastomer-Driven Long-Wave Infrared Alvarez Lenses for Continuous Zooming Imaging. *Infrared Phys. Technol.* **2024**, *143*, 105614. [CrossRef]
- 92. Zhang, Q.; Yu, W.; Zhao, J.; Meng, C.; Guo, S. A Review of the Applications and Challenges of Dielectric Elastomer Actuators in Soft Robotics. *Machines* **2025**, *13*, 101. [CrossRef]
- 93. Banet, P.; Zeggai, N.; Chavanne, J.; Nguyen, G.T.M.; Chikh, L.; Plesse, C.; Almanza, M.; Martinez, T.; Civet, Y.; Perriard, Y.; et al. Evaluation of Dielectric Elastomers to Develop Materials Suitable for Actuation. *Soft Matter* **2021**, *17*, 10786–10805. [CrossRef] [PubMed]
- 94. Jiang, S.; Tang, C.; Liu, X.-J.; Zhao, H. Long-life-cycle and Damage-recovery Artificial Muscles via Controllable and Observable Self-clearing Process. *Adv. Eng. Mater.* **2022**, *24*, 2101017. [CrossRef]
- 95. Jiang, S.; Peng, J.; Wang, L.; Ma, H.; Shi, Y. Recent Progress in the Development of Dielectric Elastomer Materials and Their Multilayer Actuators. *J. Zhejiang Univ.-Sci. A* **2024**, 25, 183–205. [CrossRef]
- 96. Ma, W.; Wang, H.; Sun, W.; Tang, C.; Cao, C.; Gao, X.; Liu, L.; Li, B.; Chen, G. Use of a multilayered dielectric elastomer actuator as a high-performance artificial muscle. Design, fabrication, and applications. *SCI. SIN. Phys. Mech. Astron.* **2024**. (In Chinese) [CrossRef]
- 97. Kim, S.; Hsiao, Y.-H.; Lee, Y.; Zhu, W.; Ren, Z.; Niroui, F.; Chen, Y. Laser-Assisted Failure Recovery for Dielectric Elastomer Actuators in Aerial Robots. *Sci. Rob.* **2023**, *8*, eadf4278. [CrossRef]
- 98. Beco Albuquerque, F.; Shea, H.R. Effect of Electrode Composition and Patterning Method on the Lifetime of Silicone-Based Dielectric Elastomer Actuators (DEA) under Different Environmental Conditions. In *Electroactive Polymer Actuators and Devices* (EAPAD) XXIII, Proceedings of the SPIE Smart Structures + Nondestructive Evaluation, San Diego, CA, USA, 22–27 March 2021; Madden, J.D., Anderson, I.A., Shea, H.R., Eds.; SPIE: San Diego, CA, USA, 2021; pp. 155–166.
- 99. Guo, Y.; Qin, Q.; Han, Z.; Plamthottam, R.; Possinger, M.; Pei, Q. Dielectric Elastomer Artificial Muscle Materials Advancement and Soft Robotic Applications. *Smartmat* **2023**, *4*, e1203. [CrossRef]
- 100. Hill, M.; Rizzello, G.; Seelecke, S. Development and Validation of a Fatigue Testing Setup for Dielectric Elastomer Membrane Actuators. *Smart Mater. Struct.* **2019**, *28*, 55029. [CrossRef]
- 101. Zhou, S.; Yu, C.; Chen, M.; Shi, C.; Gu, R.; Qu, D. Self-healing and Shape-shifting Polymers Controlled by Dynamic Bonds. *Smart Mol.* 2023, 1, e20220009. [CrossRef]
- 102. Yuan, W.; Brochu, P.; Ha, S.M.; Pei, Q. Dielectric Oil Coated Single-Walled Carbon Nanotube Electrodes for Stable, Large-Strain Actuation with Dielectric Elastomers. *Sens. Actuators A Phys.* **2009**, *155*, 278–284. [CrossRef]
- 103. Stoyanov, H.; Brochu, P.; Niu, X.; Lai, C.; Yun, S.; Pei, Q. Long Lifetime, Fault-Tolerant Freestanding Actuators Based on a Silicone Dielectric Elastomer and Self-Clearing Carbon Nanotube Compliant Electrodes. *RSC Adv.* **2013**, *3*, 2272. [CrossRef]
- 104. Annapooranan, R.; Wang, Y.; Cai, S. Harnessing Soft Elasticity of Liquid Crystal Elastomers to Achieve Low Voltage Driven Actuation. *Adv. Mater. Technol.* **2023**, *8*, 2201969. [CrossRef]
- 105. Lv, J.; Hong, H.; Gan, Z.; Zhang, M.; Liu, Z.; Hu, Z. Dielectric Elastomer-Driven Liquid Prism Enabling Two-Dimensional Beam Control. *Opt. Express* **2024**, *32*, 21517. [CrossRef]
- 106. Zhang, X.; Xu, H.; Chen, X.; Li, Z.; Su, C.-Y. Modeling and Adaptive Output Feedback Control of Butterfly-like Hysteretic Nonlinear Systems with Creep and Their Applications. *IEEE Trans. Ind. Electron.* **2023**, *70*, 5182–5191. [CrossRef]
- 107. Lv, J.; Hong, H.; Zhang, M.; Gan, Z.; Liu, Z.; Hu, Z.; Yang, M. Bio-Inspired Optofluidic Focus-Tunable Imaging System with Large Two-Dimensional Field-of-View Tuning Capability. *Measurement* 2025, 253, 117332. [CrossRef]
- 108. Medina, H.; Farmer, C.; Liu, I. Dielectric Elastomer-Based Actuators: A Modeling and Control Review for Non-Experts. *Actuators* **2024**, *13*, 151. [CrossRef]
- 109. Wang, Y.; Huang, P.; Wu, J.; Su, C.-Y. Modelling and Compound Control of Intelligently Dielectric Elastomer Actuator. *Control Eng. Pract.* **2022**, *126*, 105261. [CrossRef]
- 110. Papaspiridis, F.G.; Antoniadis, I.A. Dielectric Elastomer Actuators as Elements of Active Vibration Control Systems. *Adv. Sci. Technol.* **2009**, *61*, 103–111.

111. Wang, Y.; Zhang, X.; Li, Z.; Chen, X.; Su, C.-Y. Adaptive Implicit Inverse Control for a Class of Butterfly-Like Hysteretic Nonlinear Systems and Its Application to Dielectric Elastomer Actuators. *IEEE Trans. Ind. Electron.* **2023**, *70*, 731–740. [CrossRef]

- 112. Zhang, Y.; Wu, J.; Huang, P.; Su, C.-Y.; Wang, Y. Inverse Dynamics Modelling and Tracking Control of Conical Dielectric Elastomer Actuator Based on GRU Neural Network. *Eng. Appl. Artif. Intell.* **2023**, *118*, 105668. [CrossRef]
- 113. Yu, W.; Chen, W.; Yuan, W.; Li, G.; Meng, C.; Guo, S. Ultrathin and Highly-Stable Rubber Electrodes Based on Island-Bridge Multi-Filler Conductive Network for Multilayer-Stacked Dielectric Elastomer Artificial Muscles. *Chem. Eng. J.* 2024, 493, 152714. [CrossRef]
- 114. Liebetraut, P.; Petsch, S.; Zappe, H. A Versatile Fabrication Process for Reaction Injection Molded Elastomeric Micro-Lenses. In Proceedings of the 2012 International Conference on Optical MEMS and Nanophotonics, Banff, AB, Canada, 6–9 August 2012; IEEE: New York, NY, USA, 2012; pp. 176–177.
- 115. Zhang, H.; Zhu, J.; Wen, H.; Xia, Z.; Zhang, Z. Biomimetic Human Eyes in Adaptive Lenses with Conductive Gels. *J. Mech. Behav. Biomed. Mater.* **2023**, 139, 105689. [CrossRef] [PubMed]
- 116. Hao, Q.; Liu, L.; Cao, J.; Liu, M.; Ou, Y.; Cheng, Y. Thin Wide Range Varifocal Diffractive Alvarez Lenses Actuated by Dielectric Elastomers. *Opt. Lasers Eng.* **2024**, *182*, 108453. [CrossRef]

Disclaimer/Publisher's Note: The statements, opinions and data contained in all publications are solely those of the individual author(s) and contributor(s) and not of MDPI and/or the editor(s). MDPI and/or the editor(s) disclaim responsibility for any injury to people or property resulting from any ideas, methods, instructions or products referred to in the content.